doi:10.1093/brain/awx364 BRAIN 2018: 141; 744–761 | 744

BRAIN
A JOURNAL OF NEUROLOGY

A novel metabolism-based phenotypic drug discovery platform in zebrafish uncovers HDACs 1 and 3 as a potential combined anti-seizure drug target

Kingsley Ibhazehiebo,[1,2] Cezar Gavrilovici,[2,3] Cristiane L. de la Hoz,[1,2] Shun-Chieh Ma,[4] Renata Rehak,[1,2] Gaurav Kaushik,[1,2] Paola L. Meza Santoscoy,[1,2] Lucas Scott,[2,3] Nandan Nath,[1,2] Do-Young Kim,[4] Jong M. Rho[2,3] and Deborah M. Kurrasch[1,2]

Despite the development of newer anti-seizure medications over the past 50 years, 30–40% of patients with epilepsy remain refractory to treatment. One explanation for this lack of progress is that the current screening process is largely biased towards transmembrane channels and receptors, and ignores intracellular proteins and enzymes that might serve as efficacious molecular targets. Here, we report the development of a novel drug screening platform that harnesses the power of zebrafish genetics and combines it with *in vivo* bioenergetics screening assays to uncover therapeutic agents that improve mitochondrial health in diseased animals. By screening commercially available chemical libraries of approved drugs, for which the molecular targets and pathways are well characterized, we were able to reverse-identify the proteins targeted by efficacious compounds and confirm the physiological roles that they play by utilizing other pharmacological ligands. Indeed, using an 870-compound screen in *kcna1*-morpholino epileptic zebrafish larvae, we uncovered vorinostat (Zolinza™; suberanilohydroxamic acid, SAHA) as a potent anti-seizure agent. We further demonstrated that vorinostat decreased average daily seizures by ~60% in epileptic *Kcna1*-null mice using video-EEG recordings. Given that vorinostat is a broad histone deacetylase (HDAC) inhibitor, we then delineated a specific subset of HDACs, namely HDACs 1 and 3, as potential drug targets for future screening. In summary, we have developed a novel phenotypic, metabolism-based experimental therapeutics platform that can be used to identify new molecular targets for future drug discovery in epilepsy.

1 Department of Medical Genetics, Cumming School of Medicine, University of Calgary, Calgary, Canada
2 Alberta Children's Hospital Research Institute, University of Calgary, Canada
3 Departments of Pediatrics, Clinical Neurosciences, Physiology and Pharmacology, Cumming School of Medicine, University of Calgary, Calgary, Canada
4 Departments of Neurology and Neurobiology, Barrow Neurological Institute, St Joseph's Hospital and Medical Center, Phoenix, Arizona, USA

Correspondence to: Deborah M. Kurrasch
Department of Medical Genetics
Cumming School of Medicine
3330 Hospital Drive, HSC 2215
Calgary, AB T2N 4N1, Canada
E-mail: kurrasch@ucalgary.ca

Keywords: epilepsy; drug screening; zebrafish; bioenergetics

Received March 24, 2017. Revised October 29, 2017. Accepted November 5, 2017. Advance Access publication January 24, 2018

Abbreviations: ASD = anti-seizure drug; MES = maximal electroshock seizure; MO = morpholino oligomer; PTZ = pentylenetetratrazol

Introduction

Epilepsy is a common neurological disorder that affects ~1% of the population worldwide and can arise from a genetic mutation, inflammation, neurotrauma, or brain malformations (Berg *et al.*, 1996; Linehan *et al.*, 2011; Neligan *et al.*, 2012). The defining feature of epilepsy is the presence of spontaneous recurrent seizures, which at a cellular level manifest as aberrant discharges of neuronal clusters leading to hyperexcitability and hypersynchrony. Since the 1930s, more than 35 new anti-seizure drugs (ASDs) have been approved, and a small majority of patients are able to experience seizure control (Loscher and Schmidt, 2011). However, more than a third of all patients fail to respond to current therapies (Kwan and Brodie, 2000), and will continue to have attendant life-long cognitive, behavioural and mental health problems (Bromley *et al.*, 2011; Kanner, 2013*a*, *b*; Mula, 2013; Rudzinshi and Meador, 2013). Thus, despite the advent of newer medications and decades of research into the neurobiology of epilepsy, the proportion of patients with unremitting seizure activity has remained essentially unchanged.

Intriguingly, many of these medically refractory patients will respond to a therapeutic intervention called the ketogenic diet. The ketogenic diet is a high-fat, low-carbohydrate treatment for patients who fail to respond to anti-seizure medications (Neal *et al.*, 2008, 2009; Kossoff *et al.*, 2009), and was originally designed in the 1920s to mirror the biochemical changes associated with fasting (Kossoff and Rho, 2009). The hallmark feature of the ketogenic diet is the production of ketone bodies such as β-hydroxybutyrate, acetoacetate, and acetone. Although the underlying mechanisms of ketogenic diet action remain unclear (Rogawski *et al.*, 2016), proof of clinical efficacy has been demonstrated (Neal *et al.*, 2008) and substrates such as ketone bodies have been found to exert neuroprotective effects (Gano *et al.*, 2014). Indeed, patients who respond to the ketogenic diet show underlying respiration changes (Kang *et al.*, 2007; Greco *et al.*, 2016; Rogawski *et al.*, 2016), further demonstrating a link between the ketogenic diet and alterations in bioenergetics. There is also mounting evidence that neurometabolic alterations, such as those induced by fasting or the ketogenic diet, may improve symptoms across many unrelated neurological disorders, such as Alzheimer's and Parkinson's diseases, amyotrophic lateral sclerosis, brain cancer, neurotrauma, autism spectrum disorder, depression, and stroke (Gasior *et al.*, 2006; Acharya *et al.*, 2008; Davis *et al.*, 2008; Fenoglio-Simeone *et al.*, 2009; Maalouf *et al.*, 2009; Masino *et al.*, 2009; Stafford *et al.*, 2010; Abdelwahab *et al.*, 2012; Kim do *et al.*, 2012; Stafstrom and Rho, 2012; Ruskin *et al.*, 2013). Indeed, the ketogenic diet is currently being therapeutically explored in all of these diverse models and patient populations (Yaroslavsky *et al.*, 2002; Evangeliou *et al.*, 2003; Henderson *et al.*, 2009; Kossoff and Rho, 2009; Frye *et al.*, 2011; Maggioni *et al.*, 2011; Schmidt *et al.*, 2011; Phelps *et al.*, 2012; Herbert and Buckley, 2013; Maroon *et al.*, 2013). Since derangements in cellular metabolism have been linked in part to the underlying aetiology of epilepsy, it is possible that restoration of mitochondria-mediated bioenergetics to baseline levels will not only improve symptoms, but may also have disease-modifying effects (Pathak *et al.*, 2013). Hence, the ketogenic diet can serve as a framework for drug development for a multiplicity of neurological disorders, all of which share in common imbalances in cellular bioenergetics.

Zebrafish have rapidly become a key tool in epilepsy research and experimental therapeutics (Baraban *et al.*, 2005, 2007; Baxendale *et al.*, 2012; Zdebik *et al.*, 2013). Zebrafish are simple vertebrates that are highly amenable to genetic manipulation and share >70% genetic similarity with humans (Howe *et al.*, 2013; Kettleborough *et al.*, 2013; Schier, 2013). Thus, many biological pathways are conserved between zebrafish and humans. Increased locomotor and swimming behaviours of zebrafish in monitored assays are indicative of neuronal hyperexcitability, and thus can serve as surrogate readouts for seizure-like activity (Baraban *et al.*, 2005, 2007; Afrikanova *et al.*, 2013). More recently, electrophysiological field potential recordings in zebrafish have been used to measure epileptiform-like interictal and ictal activity in living larvae (Zdebik *et al.*, 2013; Meyer *et al.*, 2016), further demonstrating a common pathophysiology of epilepsy between mammals and teleosts. Indeed, zebrafish have been used over the past 10 years to identify drugs for the treatment of Dravet syndrome (also known as severe myoclonic epilepsy of infancy) (Baraban *et al.*, 2013) and generalized epilepsies (Baxendale *et al.*, 2012).

Here, we build upon this literature and report the characterization of a novel, metabolism-based drug discovery platform modelled on one of the mechanistic underpinnings (e.g. mitochondrial changes) and therapeutic efficacy of the ketogenic diet. We reasoned that since the ketogenic diet often works when ASDs fail, pharmacological agents that exert similar neurometabolic effects might prove as or more efficacious as existing medications. Specifically, we used a combination of zebrafish genetics and *in vivo* bioenergetics functional readout assays to screen for therapeutic agents that improve mitochondrial health in single-gene knockdown models of epilepsy. We screened commercially available chemical libraries of approved drugs, for which the molecular targets and pathways are well characterized, and confirmed the reverse-identified targets of efficacious

compounds by utilizing other pharmacological ligands. Through this process, we identified two histone deacetylases (HDAC1 and HDAC3) as selective targets for epilepsy drug development.

Materials and methods

Zebrafish husbandry and embryo culture

All protocols and procedures were approved by the Health Science Animal Care Committee (protocol number AC14-0223) at the University of Calgary in compliance with the Guidelines of the Canadian Council of Animal Care. Adult wild-type zebrafish (TL strain) were maintained at 28°C in a 14-h light/10-h dark cycle in a self-regulating aquatic system (Tecniplast) with pH 7.5–8.0, and a water conductivity of 980—1000 µS/cm, a modification of the protocol described by Westerfield (2000). The animals were fed twice daily with artemia. The evening prior to the day of breeding, breeding pairs were placed in a partitioned breeding tank (Tecniplast) to prevent egg predation. The next morning, spawning was triggered by the onset of light and removal of the partition. Zebrafish embryos and larvae were maintained in a non-CO_2 incubator (VWR) at 28°C on the same light-dark cycle as the aquatic facility.

Morpholino analyses

As the zebrafish *kcna1a* gene comprises a single exon, an ATG-blocking morpholino oligomer (MO) was engineered by Gene-Tools (Philomath). This morpholino (5′-GTTGTCCCC AGCCACAACTGTCATC-3′), denoted as *kcna1a*-MO* in Supplementary Fig. 1A and B, was the primary MO utilized throughout this project and is hereafter referred to as '*kcna1*-MO'. To verify selectivity of *kcna1a*-MO*, a second MO (5′-TGCAGGTCAAAGTTGAAGCTCCGCA-3′) was engineered by Gene-Tools to target just upstream of the first sequence (Supplementary Fig. 1A, '*kcna1a*-MO'). Additionally, a p53-targeting MO (Gene-Tools) was also co-injected with both *kcna1*-MOs to verify that the observed *kcna1*-MO phenotype was not the result of these MOs having off-target effects on the apoptotic pathway (Supplementary Fig. 1B). Both *kcna1a* ATG-blocking MOs were confirmed *in silico* to not bind *kcna1b*. For all experiments, embryos were injected at the one-cell stage, sorted, and viable embryos were maintained in 100 mm plastic petri dishes, with *kcna1*-MO and wrapped in aluminium foil, whereas wild-type embryos to be used for pentylenetetratrazol (PTZ) treatments were exposed to normal 14-h light/10-h dark cycling, and all embryos were maintained in a non-CO_2 incubator (VWR) at 28°C until the day of assay.

Drug dilution

A 142-drug library (kind gift from Dr Aru Narendran, University of Calgary) containing 10 mM compounds in dimethysulfoxide (DMSO) and a 728-compound library from the NIH containing 10 mM compounds in DMSO were used in our drug screen. On the day of assay, stock solutions of compounds were diluted to a final concentration of 20 µM in embryo media. The final DMSO concentration was 0.1%, and was used as vehicle control in behaviour assays, metabolic measurements, and zebrafish field potential recordings. For implant surgery and mouse video-EEG, vorinostat was dissolved in DMSO to a final concentration of 40 mg/kg body weight and the other compounds in a cocktail of DMSO:polyethylene glycol 300:PBS in a percentage ratio of 3.5:52:44.5 to a final concentration of 50 mg/kg body weight (Entinostat) and 100 mg/kg body weight (RG2833). Vehicle solutions for the vorinostat experiments were 10% DMSO (Fig. 6B) and DMSO:polyethylene glycol 300:PBS (see above) for entinostat and RG2833 (Fig. 7B). For the blinded study, drugs were diluted to a working concentration of 10 mM, coded, and handed to a research associate in the lab who was unable to decipher the code for each drug. This research sssociate would then run all behavioural and bioenergetics assays labelling the data using the code, and also analyse all data blindly. After data analyses were complete, the code was revealed and the data unblinded.

Behavioural assay

For drug screening using *kcna1* morphants, 5 days post-fertilization (dpf) larval zebrafish maintained in 96-well plates were habituated for 20 min, under ambient light. This was followed by treatment with 20 µM of drugs for 20–30 min ($n = 6$–7 per compound), and assayed for locomotor activity, burst activity, distance moved, inactive duration and tracking in dark for 20 min in ZebraBox (ViewPoint Life Sciences). For drug screening involving PTZ induction, 5 dpf zebrafish were treated with 10 mM PTZ for 10 min, followed by 20 µM (final concentration) of drug for 20 min under ambient light, and assayed for total locomotor activity, burst activity, distance moved and inactive duration, and tracking under 100% light in ZebraBox for 20 min. All behavioural assays were repeated at least twice. Total swim activity and tracking of total distance moved as a measure of hyperactive swimming behaviour were analysed using ZebraLab V3 software (ViewPoint Life Sciences, Lyon, France).

Metabolic measurements

Oxygen consumption rate measurements were performed using the XF24 Extracellular Flux Analyzer (Seahorse Biosciences). Single 2–4 dpf zebrafish larvae ($n = 6$–7 per group) were placed in 20 of 24 wells on an islet microplate and an islet plate capture screen was placed over the measurement area to maintain the larvae in place. Seven measurements were taken to establish basal rates, followed by treatment injections and 18 additional cycles (Stackley *et al.*, 2011). Rates were determined as the mean of two measurements, each lasting 2 min, with 3 min between each measurement (Richon, 2010).

Zebrafish electrophysiology

Electrophysiological recordings in zebrafish larvae were performed as previously described (Baraban *et al.*, 2005, 2013; Afrikanova *et al.*, 2013). Briefly, 6 dpf zebrafish were paralysed (α-bungarotoxin, 1 mg/ml, Tocris) and embedded in 1.2% low melting point agarose. The dorsal side of the zebrafish was exposed to the agarose gel surface and accessible for electrode placement. Larvae zebrafish were placed on an upright stage of

a Zeiss Axioskop2 microscope, visualized using a 5× Zeiss N-Achroplan objective and perfused with embryo media (E3 media). A glass microelectrode (3–8 MΩ) filled with 2 M NaCl was placed into the tectum opticum of zebrafish, and recording was performed in current-clamp mode, low-pass filtered at 1 kHz, high-pass filtered at 0.1 Hz, using a digital gain of 10 (Multiclamp 700B amplifier, Digidata 1440A digitizer, Axon Instruments) and stored on a PC computer running pClamp software (Axon Instruments). After 20 min of baseline recording, drugs (final concentration 20 μM) were added directly to the embryo media and continued recordings in the same fish were captured over the next 20 min. Care was taken not to disrupt the pipette or move the fish in any manner.

Implant surgery and mouse video-EEG

Kcna1-null mice were anaesthetized with 3% isoflurane, and the skull fixated with stereotaxic bars (KOPF Instruments) over heating pads (as approved in Animal protocol # AC 13-0251). A 1.5 cm rostral-caudal incision was made to expose the skull surface, and connective tissues cleared. Three holes were gently drilled on each side of the skull with a 23 mm gauge needle, avoiding suture lines. Mouse screws (0.1 inch) with wire leads were gently inserted midway into the skull, and a layer of dental acrylic applied over the screw heads and skull. A 6-pin mouse connector (Pinnacle Technology) was positioned over the screws, wires properly aligned, wrapped together, and folded backwards to avoid accidental contacts. A pocket for two EMG electrodes was made in the neck of the mouse by blunt dissection. Exposed wires were covered with a final layer of dental acrylic, and allowed to harden for 24 h before attaching the pin connector to the video EEG monitor (Pinnacle Technology). EEG signals were recorded simultaneously across the rostral, medial and caudal aspects of the neocortex using Sirenia Acquisition software (Pinnacle Technology). Mice were recorded 24 h per day for 1 day (baseline, post-natal Day 38), and received vorinostat and other drugs (intraperitoneal injection, 40–100 mg/kg body weight/day) for the next six consecutive days (post-natal Days 39–44). Frequency, duration, and time of seizure was analysed using Sirenia Seizure software (Pinnacle Technology).

Psychomotor and maximal electroshock seizure testing

The 6 Hz 44-mA psychomotor and maximal electroshock seizure (MES) testing were performed as previously described (Suzuki *et al.*, 1992, 1995; Bouilleret *et al.*, 1999; Riban *et al.*, 2002; Barton *et al.*, 2003). Briefly, for the 6 Hz 44-mA psychomotor testing, 44 mA current was delivered through corneal electrodes for 3 s to CF-1 mice ($n = 4$) to elicit psychomotor seizure, while in the MES test, 60 Hz of alternating current (50 mA) was delivered for 0.2 s by corneal electrodes previously primed with an electrolyte solution containing 0.5% tetracaine HCl to CF-1 mice ($n = 4$) to induce MES seizures. Vorinostat at 30, 100, and 300 mg/kg was then administered intraperitoneally and the anti-seizure activity of vorinostat was then determined at 0.5- and 2.0-h time points.

Results

Characterization of bioenergetics functional assays in zebrafish epilepsy models

The rationale for our drug screening platform is rooted in the clinical efficacy of the ketogenic diet and its ability to modulate mitochondrial bioenergetics. Thus, first we sought to demonstrate that bioenergetics was altered in epileptic models of zebrafish. We used the Seahorse XF Flux Bioanalyzer, which enables non-invasive and real-time measurements of metabolic changes in zebrafish larvae (Fig. 1A) (Stackley *et al.*, 2011; Gibert *et al.*, 2013; Kumar *et al.*, 2016). Specifically, the Seahorse platform provides a measurement of basal respiration, maximal respiration, non-mitochondrial respiration, and mitochondrial respiration due to ATP turnover and/or proton leaks (Fig. 1A), and thereby provides a full metabolic profile in a single assay. Initially we tested a range of zebrafish ages (2–7 dpf) to determine the developmental stage that yielded the highest oxygen consumption rate with least variability, and found little differences across development (data not shown). Thus, for all experiments carried out hereafter, 2 dpf zebrafish larvae were used.

We created two models of 'epileptic' zebrafish: a pharmacological induction model using PTZ, which has been shown previously to produce epileptic-like hyperexcitability in zebrafish (Baraban *et al.*, 2005), and a knockdown approach targeting the zebrafish orthologue of the human and murine potassium channel gene (*KCNA1* and *Kcna1*, respectively) encoding the delayed rectifier protein Kv1.1, using a morpholino (MO) oligonucleotide that targeted the *kcna1a* ATG initiation site (Supplementary Fig. 1A). Initially we ordered two *kcna1a* ATG-blocking MO to confirm selectivity of the observed *kcna1a* knockdown phenotypes. Being a single exon gene, we were unable to design a slice-targeting MO. Both ATG-blocking MOs (*kcna1a*-MO* and *kcna1a*-MO) and a standard control MO were injected into wild-type embryos at the one-cell stage and assayed at 3 dpf for changes in transcript levels using RT-PCR and qPCR. The two ATG-MOs displayed an equal degradation of *kcna1a* transcripts, whereas the control MO had no effects (Supplementary Fig. 1B). In addition, bioenergetic assays were conducted on 3 dpf zebrafish larvae injected with either the control MO or either of the *kcna1a*-MOs and an equal increase in basal respiration was observed in the *kcna1a* morphants but not the control larvae (Supplementary Fig. 1B). And finally, each of these *kcna1a*-MOs was co-injected with a p53-MO to confirm that this increase in basal respiration was due to targeting of the *kcna1a* gene and not off-target effects on the apoptosis pathway, the primary effector of non-selective MOs. We demonstrate an equal level of basal respiration in the p53-MO + *kcna1a*-MO zebrafish larvae, which matches

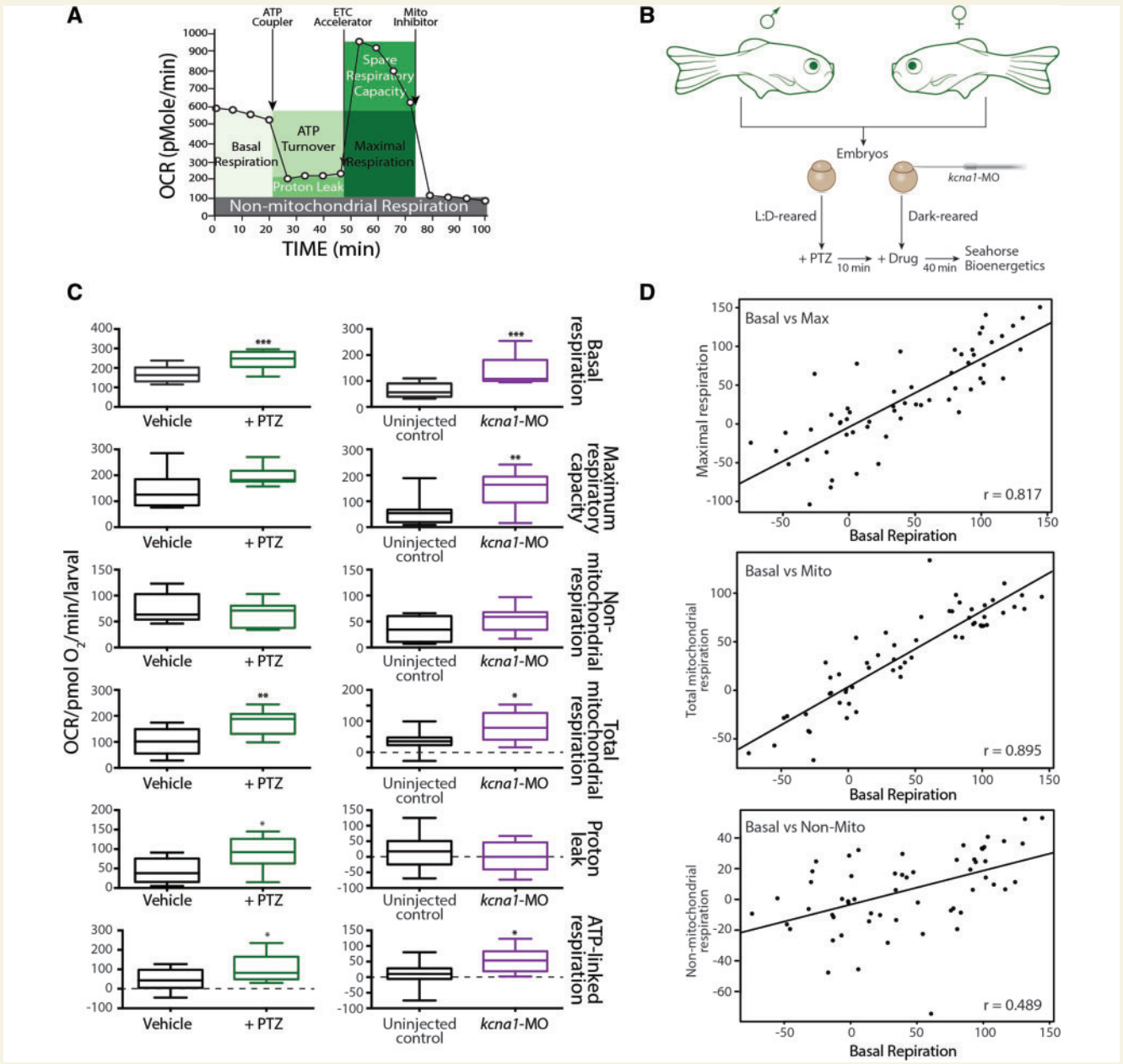

Figure 1 Metabolic characterization of PTZ and *kcna1*-MO models of epilepsy. (**A**) Cartoon representation of how the Seahorse bioanalyser displays mitochondria bioenergetics as modulated by pharmacological inhibitors. (**B**) Schematic representation of treatment paradigm for metabolic drug screen in PTZ and *kcna1*-MO models of epilepsy. (**C**) PTZ and *kcna1*-MO models of epilepsy exhibit significant increases in metabolic parameters. Specifically, changes in basal respiration, maximal respiratory capacity, non-mitochondria respiration, total mitochondrial respiration, proton leaks, and ATP-linked respiration were studied for both models. Non-mitochondrially mediated changes in respiration were not observed in either model. (**D**) Linear regression analyses showing significant correlation between basal respiration and both maximum respiratory capacity (r = 0.817; $P < 0.0001$) and mitochondria-mediated respiration (r = 0.895; $P < 0.0001$) but only a moderate correlation with non-mitochondrial respiration (r = 0.489; $P < 0.001$). Data in **C** are shown as mean ± SEM; $^{*}P < 0.05$, $^{**}P < 0.001$, $^{***}P < 0.0001$ (unpaired *t*-test); $n = 6–7$ fish per group.

kcna1a morphant levels alone (Supplementary Fig. 1B). There are two *kcna1* paralogues in zebrafish (*kcna1a* and *kcna1b*) and both *kcan1a*-MOs are 100% selective to *kcna1a*. For the rest of this study, only the *kcna1a*-MO* was used and is hereafter referred to as '*kcna1*-MO'.

Our workflow was to breed male and female wild-type zebrafish and either grow the embryos in normal light:dark cycle conditions until day of experiment and then expose them to PTZ 10 min prior to assay, or inject with MO at the one-cell stage and then allow them to grow in the dark until the day of testing (Fig. 1B–D). To validate our *kcna1*-MO epilepsy model, we examined locomotor behaviours by quantifying movement across different experimental conditions [Supplementary Fig. 1C and D; as described previously (Baraban *et al.*, 2005)]. Notably, there were no significant changes in total locomotor behaviour between *kcna1*-MO

and wild-type when reared under a 14-h light:10-h dark environment and then assayed in both dark, light, or flashing light conditions (Supplementary Fig. 1D). By contrast, when *kcna1*-MO were reared in complete dark until 5 dpf and then assayed in dark, the morphants displayed hyperactivity (Supplementary Fig. 1C and D), which was not observed in dark-reared morphants assayed under light or flashing lights (Supplementary Fig. 1D). Upon further characterization, the 5 dpf *kcna1*-MO embryos reared and assayed both in dark exhibited hyperactive swimming across all behavioural parameters examined, including increased total locomotor activity (the sum of all movements made), burst activity (a potential measure of seizure events), total distance moved, and inactive duration (Supplementary Fig. 3) (Baraban *et al.*, 2005). Notably, *kcna1*-MO showed comparable levels of locomotion as the PTZ-induction model (Supplementary Fig. 3). Finally, to demonstrate that the *kcna1*-MOs displayed neuronal hyperexcitability consistent with a seizure model, we assessed EEG activity through extracellular field recordings. Indeed, 5 and 6 dpf *kcna1*-MO exhibited abnormal EEG activity, evidenced by repetitive high frequency, large-amplitude spikes (Supplementary Fig. 2). In addition, by enlarging a section of the trace, we observe ictal (>1000 ms in duration) and interictal (<300 ms duration) -like activity, consistent with epileptiform events (Supplementary Fig. 2). Here, we define epileptiform events as upward or downward deflections greater than 2× baseline levels, as has been done previously (Baraban *et al.*, 2013). Combined, these findings are in agreement with others who have demonstrated abnormal swimming behaviour in larval 'epileptic' zebrafish models (Baraban *et al.*, 2005; Winter *et al.*, 2008; Afrikanova *et al.*, 2013; Dinday and Baraban, 2015; Grone *et al.*, 2016).

To measure bioenergetics in living zebrafish, we seeded 2 dpf wild-type embryos for induction with PTZ or *kcna1*-MO into islet capture plates and secured them under a mesh chamber to keep the larvae contained in the centre of the plate for accurate measurement. On the day of assay, wild-type embryos were treated with PTZ (10 mM) 10 min prior to the assay and PTZ-treated and *kcna1*-MO larvae (2 dpf) were placed in the extracellular flux analyser (Seahorse Bioscience). The oxygen consumption rate in a transient micro-chamber was measured over 2 min in the presence or absence of pharmacological inhibitors to block various steps in energy production (Fig. 1A) (Stackley *et al.*, 2011). In both epilepsy zebrafish models, a significant increase in core bioenergetics parameters was observed. Specifically, basal respiration, total mitochondrial respiration, and ATP-linked respiration, were elevated in both the PTZ-induction and *kcna1*-MO models (Fig. 1C; $P < 0.0001$, $n = 6$–7). In addition, maximum respiratory capacity (*kcna1*-MO only) and respiration due to proton leaks (PTZ-induction only) were also significantly increased (Fig. 1C; $P < 0.001$ and $P < 0.05$, respectively). Non-mitochondrial respiration was unchanged in both zebrafish epilepsy models, consistent with the notion that mitochondrial alterations are associated with the hyperexcitable phenotypes observed in both models (Supplementary Figs 1 and 3).

We also asked whether basal respiration in *kcna1*-MO correlated with maximal respiration, mitochondria-mediated respiration, and non-mitochondria-mediated respiration, to ascertain if basal respiration could be used as a representative readout for mitochondria-mediated events during drug screening. Using linear regression analyses, we showed a very strong correlation between basal respiration and both maximum respiratory capacity ($r = 0.817$; $P < 0.0001$) and mitochondria-mediated respiration ($r = 0.895$; $P < 0.0001$). However, only a moderate correlation with considerable variability was observed between basal respiration and non-mitochondrial respiration ($r = 0.489$; $P < 0.001$), demonstrating that basal respiration is a very poor predictor for non-mitochondrially-mediated respiration, as expected (Fig. 1D).

Anti-seizure drugs block elevated metabolism in zebrafish epilepsy models

Next, we used our two models of epilepsy to characterize the efficacy of currently approved ASDs for blocking elevated metabolism. To do so, we conducted a blind screen of 20 known ASDs plus three compounds that recently failed clinical trials in epilepsy for missed endpoints. All 23 compounds were blinded and assayed through our metabolism-based platform. As expected, we observed an increase in basal respiration in both PTZ-induction and *kcna1*-MO epilepsy models (Fig. 2A). Additionally, in the PTZ-induction zebrafish, we found 14 of 20 ASDs (including topiramate, vigabatrin, and tiagabine) potently reduced elevated basal respiration and total mitochondria respiration to wild-type levels, whereas in the *kcna1*-MO zebrafish 15 ASDs, including eslicarbazepine, rufinamide, primidone, effectively restored core bioenergetics parameters of basal respiration, maximum respiratory capacity, and total mitochondrial respiration to wild-type levels (Fig. 2A and B). Moreover, 11 of the 20 ASDs were effective in both models. In contrast, two of the 'failed' drugs were efficacious in the PTZ-induction model but none were effective in the *kcna1*-MO (Fig. 2B). Given that more ASDs were effective in the *kcna1*-MO than in the PTZ-induced zebrafish, and also since none of the failed drugs demonstrated potency in the *kcna1*-MO, it is possible that genetic models of epilepsy might offer better translatability than acute induction models. Combined, our screening platform uncovered 18 of 20 ASDs (excluding only piracetam and ethosuximide), yielding a 90% confidence rate and highlighting the robustness and utility using metabolic readouts as an approach to uncover novel ASDs.

Semi high-throughput screen of two repurposed drug libraries

Having validated metabolism as a robust readout assay in zebrafish larval epilepsy models, we next conducted a

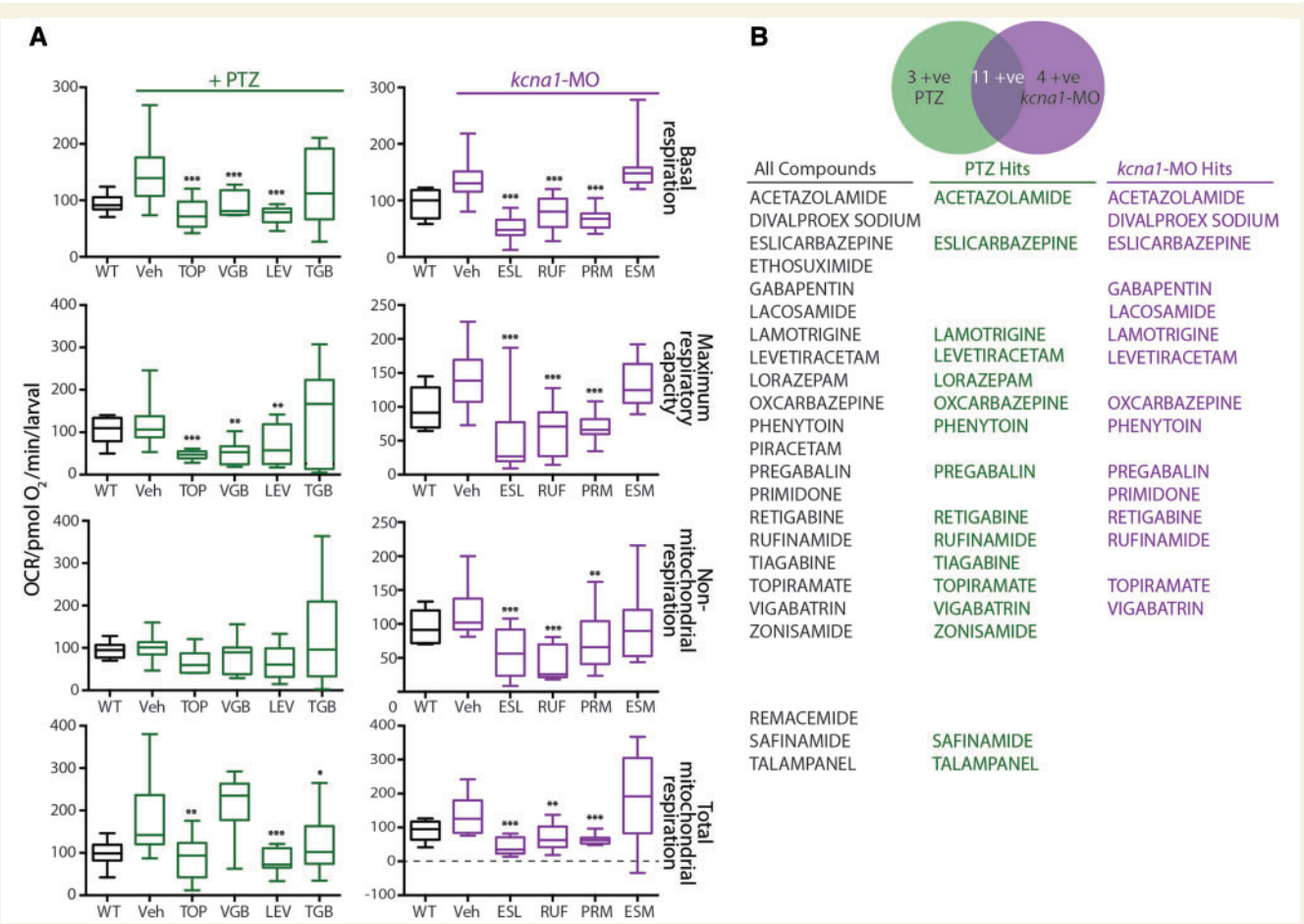

Figure 2 ASDs are efficacious in zebrafish bioenergetics assays. (**A**) A double-blinded screen of 20 known ASDs and three compounds that recently failed clinical trials in epilepsy. Thirteen of 20 known ASDs restored elevated basal respiration and total mitochondria respiration to wild-type levels in PTZ-induction model. In the *kcna1*-MO model, 15 of the 20 known ASDs were efficacious in restoring basal respiration, maximum respiratory capacity and total mitochondrial respiration to wild-type levels. (**B**) List of the 20 known ASDs and three compounds that recently failed clinical trials in epilepsy used in present study. Two of the three compounds that failed were efficacious in the PTZ-induction but not in the *kcna1*-MO model. Data in **A** are shown as mean ± SEM. Statistics are shown comparing treatment group to vehicle control; wild-type and vehicle are statistically different in all graphs although not illustrated; $*P < 0.05$, $**P < 0.001$, $***P < 0.0001$ (unpaired *t*-test); $n = 6–7$ fish per group. ESL = eslicarbazepine; ESM = ethosuximide; LEV = levetiracetam; PRM = primidone; RUF = rufinamide; TGB = tiagabine; TOP = topiramate; Veh = vehicle; VGB = vigabatrin; WT = wild-type.

two-step screen. Our workflow (Fig. 3A) was to create the zebrafish models of epilepsy, as described above, conduct a high-throughput behavioural screen to identify active compounds, and then test promising hits in the semi high-throughput metabolic assay. All positive hits were then validated in *Kcna1*-null mice (see below) and new molecular targets reverse-identified.

We used two repurposed libraries for our screen: a private library of 142 oncogenic therapies (a kind gift from Dr A. Narendren, University of Calgary) and the 728 compound NIH Clinical Collection. All 870 compounds were first screened for their ability to significantly reduce hyperactive swimming behaviours in both PTZ-induced and *kcna1*-MO zebrafish larvae. Drugs were assayed at 20 µM, slightly higher than screens conducted in tissue culture to account for lower *in vivo* uptake of the drugs. A compound was considered a positive hit if it reduced total locomotor activity by 40% or more with little or no toxic effects, as determined by the presence of normal heartbeat before and after assay, absence of pericardial oedema, and return of zebrafish to normal swimming after washout of the drug. To statistically assess the robustness of our primary screen, upon completion of the 870 compounds we created a z-score scatter plot, which represents a theoretical mean from which standard deviations of each drug away from this theoretical mean (z-score) can be calculated to assess the statistical distribution of each drug (Fig. 3B). Thus, the further the z-score is from 0, the lower the probability of obtaining the drug data value from a theoretical distribution. Here, we show all 870 compounds as grey dots and have randomly selected 25 of our 120 hits from the behavioural screen to demonstrate their distribution (Fig. 3B, purple). We also mapped onto this grid 15 green squares that are our lead compounds after assaying

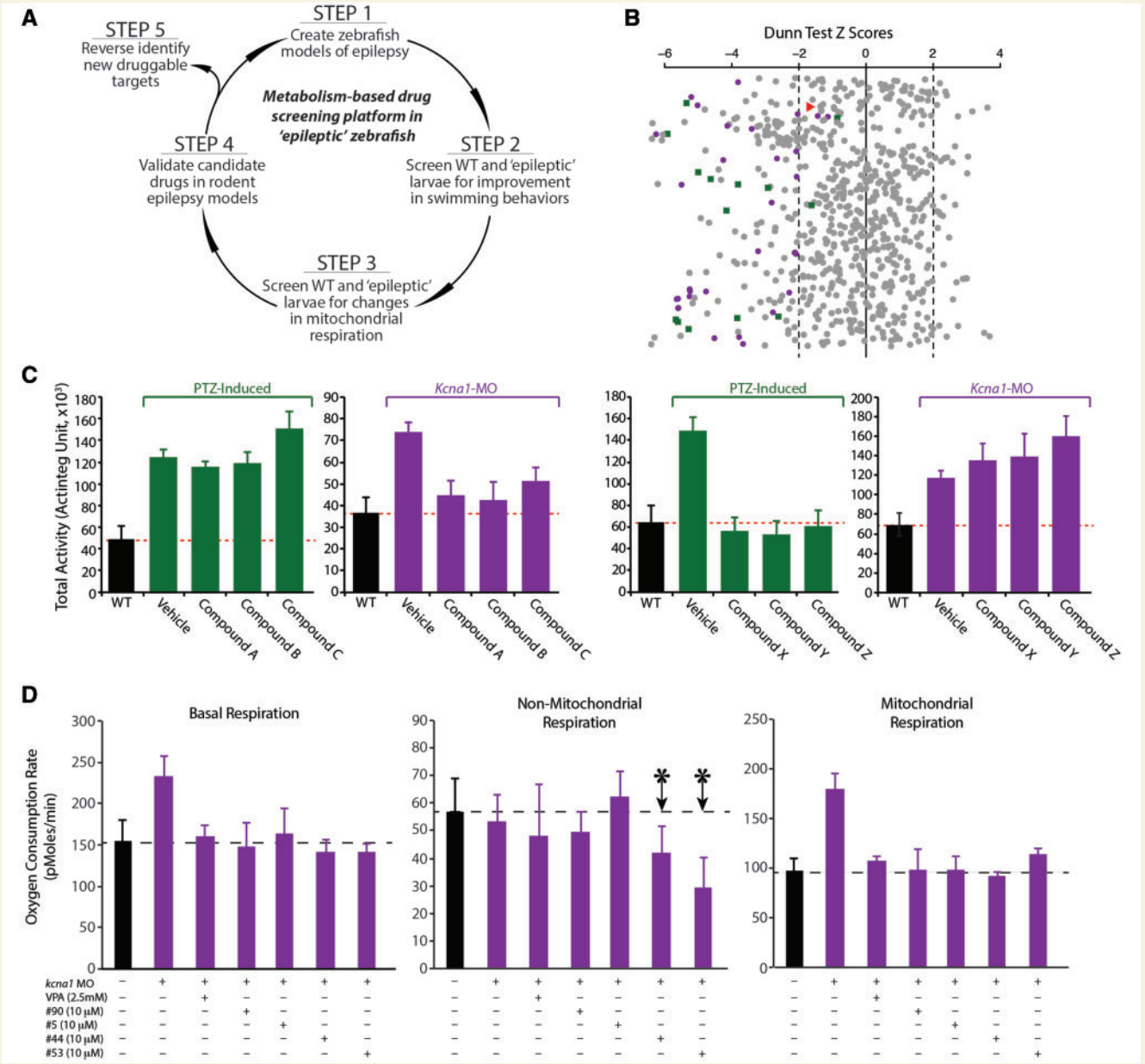

Figure 3 A screen of 870 compounds uncovers new potential ASDs. (**A**) Schematic representation of the workflow for the two-step drug screen. (**B**) Z-score scatter plot of 870 compounds used in the primary screen. Purple dots are representative hits from behavioural screen, green squares are lead compounds from both behavioural and metabolic screens. The red triangle represents vorinostat. (**C**) Identification of two categories of efficacious compounds from the behavioural screen namely; compounds effective only in *kcna1*-MO or PTZ-induction models. (**D**) Representative data showing elevated basal respiration and mitochondrially-mediated respiration in both *kcna1*-MO and PTZ-induction model is blocked by valproic acid (a known ASD) and other compounds used in drug screen including compound 53 (vorinostat), which is a broad HDAC inhibitor. Non-mitochondrial respiration is unaffected in both *kcna1*-MO and PTZ-induction models. Data in **D** are shown as mean ± SEM; $^*P < 0.001$ (unpaired *t*-test); $n = 6–7$ fish per group.

through the metabolic readouts, with vorinostat highlighted with red triangle (Fig. 3B). Combined, this analysis confirms that the cut-off of a 40% decrease in locomotor behaviour is a robust measure of efficacy since these compounds largely have a z-score < -2 ($< 5\%$ probability) when assessed using this more rigorous statistical approach.

We next examined the behavioural assay results for trends and noticed that potent compounds fell into three categories: (i) effective in *kcna1*-MO but not in the PTZ-induction model (Fig. 3C); (ii) effective in the PTZ-induction model but not in the *kcna1*-MO (Fig. 3C); (iii) effective in both models (data not shown). Only drugs that blocked high-velocity swim movements by $> 40\%$ in both models were moved forward and assessed in the semi high-throughput metabolic screen.

To assess the efficacy of these 120 compounds that passed the initial behavioural screen for improved bioenergetics,

wild-type and *kcna1*-MO zebrafish were seeded into the islet plates and exposed to PTZ and/or drug (20 μM) as described above (Fig. 1B). Although linear regression analysis demonstrated that basal respiration would suffice as a measure of metabolic activity (Fig. 1D), we assayed the entire bioenergetics profile since we desired a complete dataset from which to understand improvements in metabolism in the presence of drugs. All compounds that reversed basal and mitochondrial respiration (>40%) in both PTZ-induction and *kcna1*-MO models were considered active and prioritized. We created a representative graph of these data demonstrating that basal respiration and mitochondria-mediated respiration, but not non-mitochondria-mediated respiration, were both elevated in the *kcna1*-MO and blocked in the presence of valproate (as a control) or by compounds from the libraries (Fig. 3D). Some drugs also demonstrated an effect on non-mitochondria-mediated respiration (Fig. 3D, arrows). Notably, compound 53 is vorinostat, a broad HDAC inhibitor that significantly ameliorated the altered bioenergetics profile to wild-type levels (including basal respiration and mitochondria respiration) in both PTZ-induced and *kcna1*-MO epileptic models (Fig. 3D).

Comparative efficacy between the behavioural and bioenergetics screening assays

During our workflow from the behavioural screen through to the bioenergetics assay, we noticed a high failure rate. That is, low numbers of potential leads were efficacious in the metabolic screen, suggesting either a high false-positive rate from the behavioural screen and/or low utility of metabolism as a readout assay. Given that 90% of ASDs would have been discovered across our two zebrafish epilepsy models using the bioenergetics assay, we wondered if the behavioural assay was less robust. To test this notion, we repeated our blinded study and measured the efficacy of 20 ASDs in the PTZ-induced and *kcna1*-MO models (Fig. 4). Indeed, we noticed that ASDs that were efficacious in the bioenergetics assay (Fig. 4A, right column) were ineffective in the behavioural screen (Fig. 4A, left column). For example, vigabatrin, levetiracetam, and lamotrigine efficiently reduced basal and mitochondrial respiration in PTZ-induced and *kcna1*-MO models but failed to have any effects on swimming behaviours in both model's larvae (Fig. 4A). In total, we measured 12 of 20 ASDs as efficacious across both PTZ-induced and *kcna1*-MO models in the behavioural assay (60%; Fig. 4B, illustrating locomotion data only). Notably, the two drugs (ethosuximide and piracetam) not efficacious in the metabolic screen in both models, were effective in the PTZ-induction model for the behaviour assay (Fig. 4B). These results prompted us to conduct a linear regression analysis and compared total locomotor activity versus either basal or mitochondria-mediated respiration (Fig. 4C). Either a very weak negative correlation (total locomotion versus basal respiration) or no correlation (total locomotion versus total mitochondrial respiration) was observed, suggesting that behavioural and metabolic readouts are not linked.

Vorinostat is uncovered as a potential anti-seizure drug

Our top candidate after screening the initial 120 hits through the bioenergetics assay was vorinostat, which is also known as suberanilohydroxamic acid (SAHA). To fully characterize the metabolic profile of vorinostat, we examined a wide range of bioenergetics parameters, including basal respiration, maximal respiration, non-mitochondrial respiration, mitochondrial respiration, proton leaks, and ATP-linked respiration. Vorinostat was shown to be highly efficacious in reducing these parameters to wild-type levels, with the exception of non-mitochondria respiration, in both PTZ-induced and *kcna1*-MO epilepsy models (Fig. 5A; unpaired *t*-test, basal respiration $P < 0.0001$, maximum respiratory capacity $P < 0.001$, total mitochondrial respiration $P < 0.0001$, proton leaks $P < 0.001$, and ATP-linked respiration $P < 0.05$). We found the effective dose to be in the range of 20 to 50 μM (Fig. 5B), with higher doses of vorinostat (100–300 μM) toxic to zebrafish larvae, as demonstrated by lethargic swimming and reduced heart rate, as well as eventual death at continued exposure to highest doses (data not shown).

Vorinostat reduces seizure activity in epileptic zebrafish larvae and rodent models

To determine if vorinostat functions as an effective ASD, we used three models: (i) extracellular field recordings in zebrafish; (ii) video-EEG recordings in mice; and (iii) acutely-induced approaches in mice [in collaboration with the United States National Institutes of Health-sponsored Epilepsy Therapy Screening Program (ETSP)]. First, we measured extracellular field potentials from the optic tectum of paralysed and agarose-immobilized wild-type and *kcna1*-MO zebrafish brains (Fig. 6A). In wild-type zebrafish, we detected no evidence of abnormal electrical discharges, whereas field recordings in *kcna1*-MO larvae revealed repetitive high-frequency, large-amplitude spikes indicative of hyperexcitability (Fig. 6A and Supplementary Fig. 1). Perfusion of *kcna1*-MO with vorinostat (40 μM) for 30 min nearly completely abolished the high-frequency spikes (Fig. 6A). We next examined the efficacy of vorinostat administration on seizure frequency in spontaneously epileptic *Kcna1*-null mice lacking the delayed rectifier potassium channel α subunit, $K_v1.1$ (Fig. 6B). Treatment of these mice with vorinostat (40 mg/kg body weight/day) significantly reduced seizure frequency by 60%. Although a reduction in seizure frequency was observed as early as 24 h after commencement of treatment (Fig. 6B), it took 4 days to reach significance (Fig. 6B), consistent with the

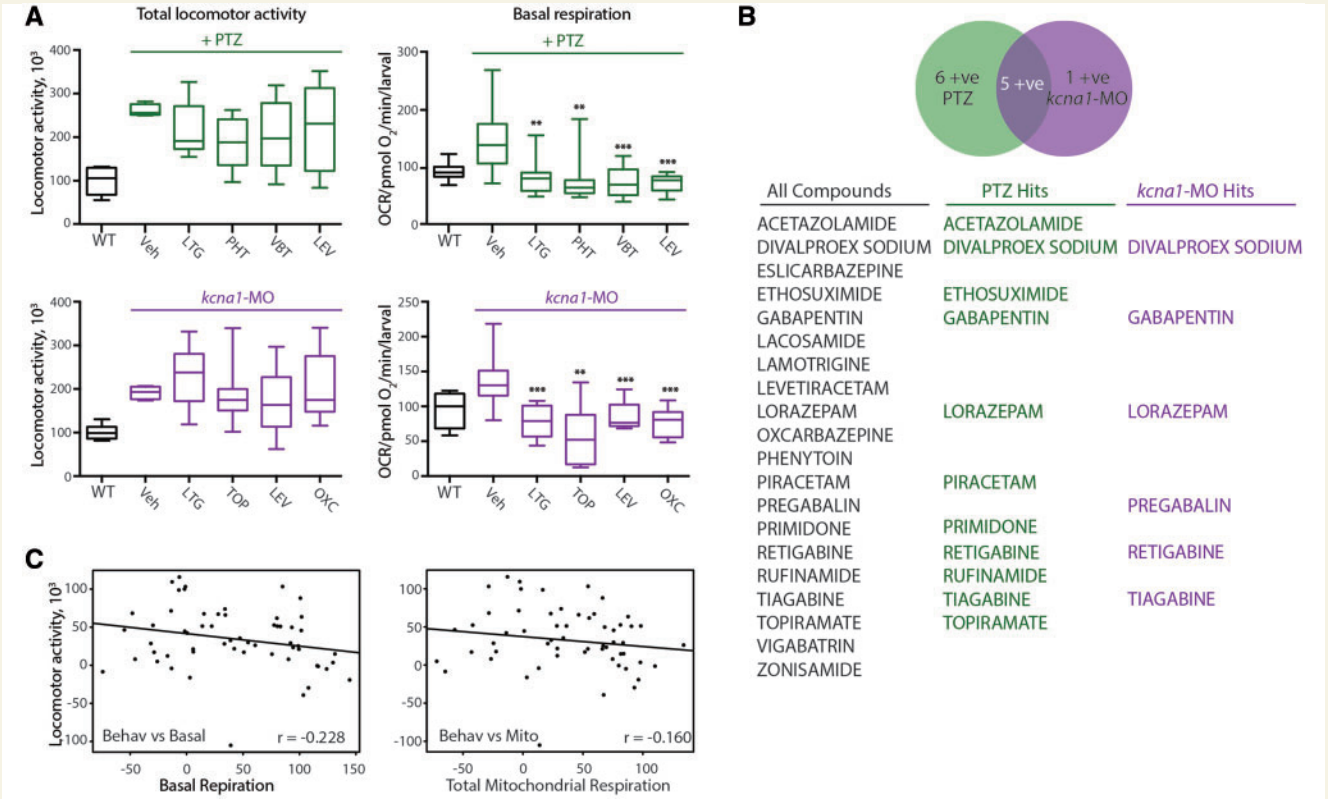

Figure 4 ASDs are less robust in behavioural assays. (**A**) Comparison between behavioural and metabolic assays indicates behavioural efficacy is not predictive of bioenergetics efficacy. Known ASDs including levetiracetam and lamotrigine that effectively reduced elevated basal and mitochondrially-mediated respiration in PTZ-induction and *kcna1*-MO models had no effect on altered swimming behaviour in both models. (**B**) List of 20 known ASDs used in the behavioural screen. Eleven of 20 ASDs were efficacious in the PTZ-induction model, 6 of 20 were effective in the *kcna1*-MO, and 5 of 20 effective in both models. Data shown are for drugs efficacious in the locomotion assay only. (**C**) Linear regression analyses indicated a very weak negative correlation between total locomotor activity and basal respiration ($r = -0.228$; $P = 0.04$) and no correlation between total locomotor activity and total mitochondrial respiration ($r = -0.160$; $P > 0.1$). Data in **A** are shown as mean ± SEM; statistics are shown comparing treatment group to vehicle control; wild-type and vehicle are statistically different in all graphs although not illustrated; $^{**}P < 0.001$, $^{***}P < 0.0001$ (unpaired *t*-test); $n = 6$–7 fish per group. LGT = lamotrigine; LEV = levetiracetam; OXC = oxcarbazepine; PHT = phenytoin; TOP = topiramate; VBT = vigabatrin; Veh = vehicle; WT = wild-type.

notion that HDAC inhibitors might require additional time to be effective. Finally, we examined the acute effect of vorinostat administration on seizures in the 6 Hz psychomotor and MES models that represent therapy-resistant limbic seizures and tonic-clonic seizures, respectively (White *et al.*, 1995; Barton *et al.*, 2001). When the animals were dosed 30 min prior to the 6 Hz test, none of the 30 mg/kg animals responded, whereas 50% and 75% responded at the 100 mg/kg and 300 mg/kg doses, respectively. However, when treated with vorinostat 2 h prior to the 6 Hz test, nearly all the animals responded at all doses (Fig. 6C). Rotarod testing also revealed toxicity at the higher doses (100 mg/kg and 300 mg/kg), which is consistent with our findings in zebrafish (data not shown). Interestingly, vorinostat was far less efficacious in the MES test, with none of the animals responding to treatment when dosed 30 min prior, and only one to two animals responding when treated 2 h prior to MES stimulation (Fig. 6C). These data suggest that vorinostat may not possess a broad-spectrum anti-seizure profile. That said, however, ASDs that are principally effective in the MES model are voltage-gated sodium channel blockers with restricted efficacy against focal-onset seizures, whereas valproic acid—having known activity as a HDAC inhibitor—is a broad-spectrum drug.

Selective inhibition of HDAC1 and HDAC3 as a novel target for anti-seizure drugs

Given that vorinostat is a broad HDAC inhibitor, we were concerned that therapeutically it might have multiple off-target effects that would reduce its utility as an anti-seizure therapy, notably with regard to adverse effects. In fact, valproic acid is a potent ASD that broadly targets class I and IIa HDACs (Gottlicher *et al.*, 2001), and it is poorly tolerated due to side effects such as weight gain and the potential for multiple organ toxicities. Therefore, we asked if we could identify a more selective HDAC inhibitor, against which future drug discovery could be targeted. To do so, we systematically analysed the bioenergetics profile of 26 HDAC inhibitors from class I, IIa, IIb, and IV in the *kcna1*-MO

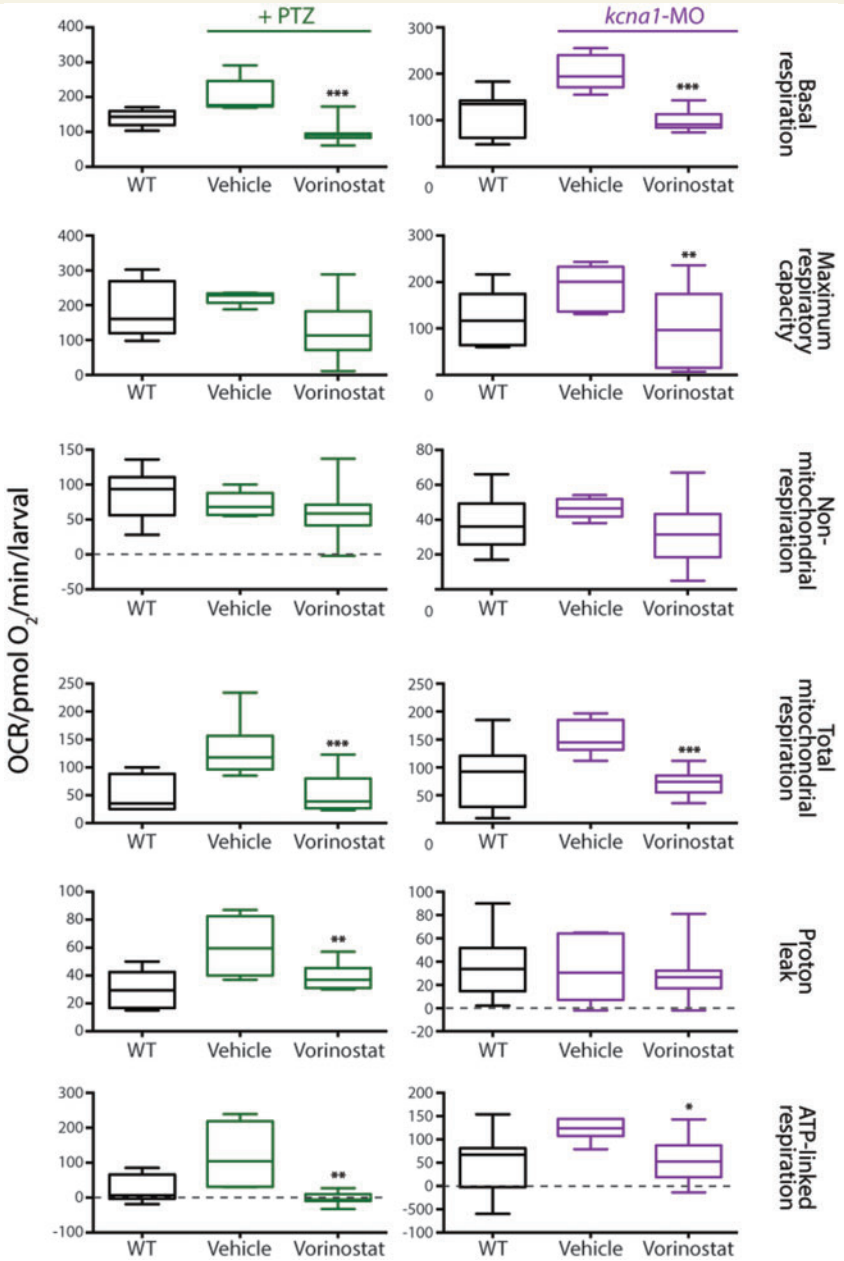

Figure 5 Vorinostat is efficacious for mitochondria-mediated respiration. Vorinostat effectively ameliorated the elevated metabolic parameters of basal respiration, maximum respiratory capacity, mitochondria respiration, proton leaks and ATP-linked respiration in both PTZ-induced and *kcna1*-MO models. Data are shown as mean ± SEM; statistics are shown comparing treatment group to vehicle control; wild-type (WT) and vehicle are statistically different in all graphs although not illustrated; $*P < 0.05$, $**P < 0.001$, $***P < 0.0001$ (unpaired *t*-test); $n = 6–7$ fish per group.

(Table 1). We screened for the ability of a particular HDAC inhibitor (40 μM) to restore the elevated basal respiration observed in *kcna1* morphants to wild-type levels. Exposure to an inhibitor selective for HDAC1 (e.g. MC1568) or for both HDAC1 and HDAC3 (e.g. etinostat, SBHA, RG2833) reduced elevated basal respiratory rates to control levels (Fig. 7A). In contrast, treatment with an inhibitor selective to HDAC3 (e.g. RGFP966) or a different HDAC1 inhibitor (e.g. tacedinaline) had no effect on the elevated basal respiration levels in *kcna1*-MO (Fig. 7A), suggesting that a combination HDAC1 and HDAC3 inhibition might be required. To further test this idea, we treated *Kcna1*-null mice with the HDAC1 and HDAC3 inhibitor RG2833 (100 mg/kg body weight/day) and showed using video-EEG that the number of seizures per day decreased by over 50% (Fig. 7B and Supplementary Fig. 3A) and that this treatment specifically decreased Stage 3 seizures without affecting low-level Stage 2 seizures (Supplementary Fig. 4B), as scored using a modified Racine scale (Fenoglio-Simeone *et al.*, 2009). Combined, these results are consistent with the

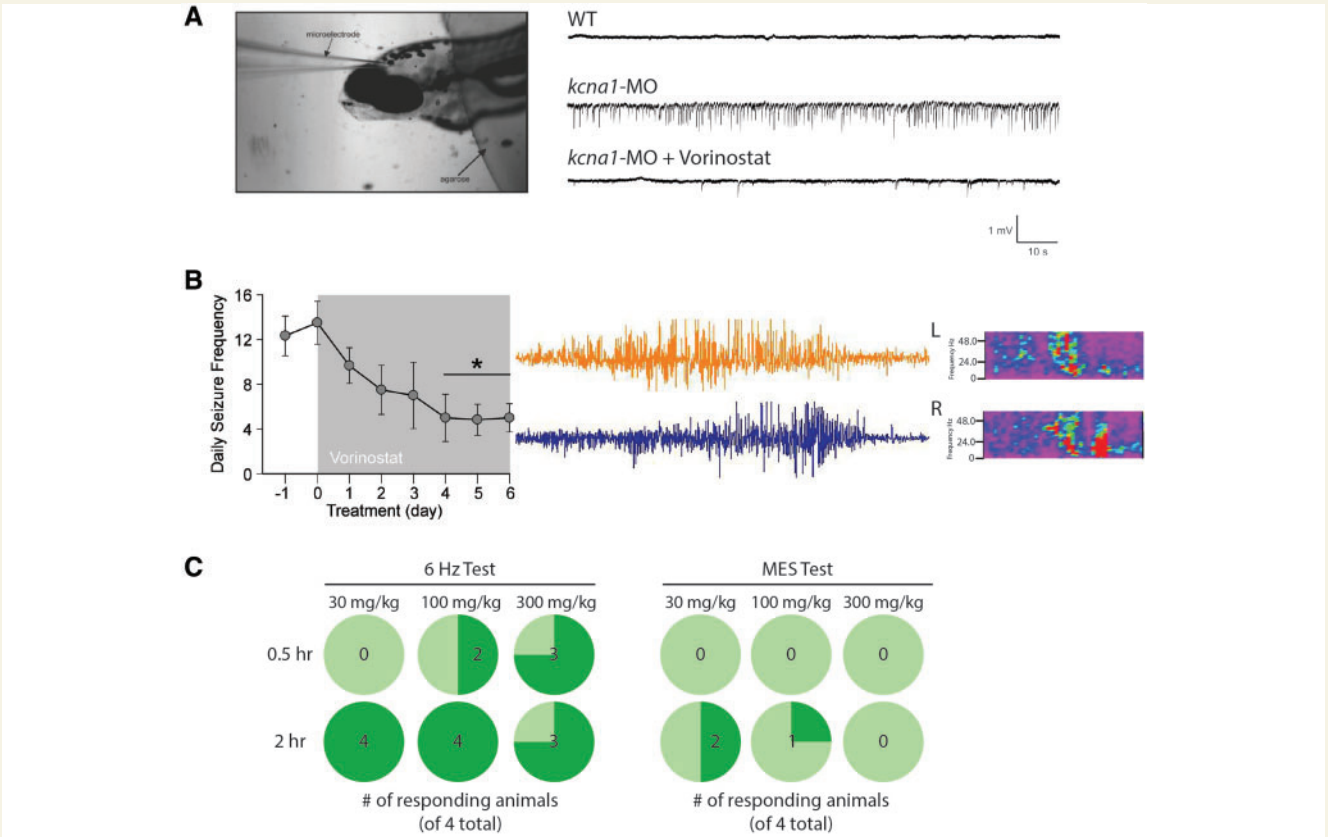

Figure 6 Vorinostat blocks seizures in zebrafish and rodents. (**A**) Image shows agarose-embedded zebrafish and the placement of a glass microelectrode in the tectum opticum. Representative extracellular field recordings obtained from the optic tectum of 6 dpf wild-type and *kcna1*-MO zebrafish larvae ± vorinostat treatment (40 μM). The presence of repetitive high frequency, large amplitude spikes indicative of hyperexcitability in knockdown animals is shown, and is abolished in the presence of vorinostat. (**B**) Representative electrographic seizure and heat maps recorded in *Kcna1*-null mice. Bar graph of the mean number of seizures per day recorded from six *Kcna1*-null mice ± vorinostat treatment. Mice were recorded for 24 h per day for 1 day, and then received vorinostat injection (40 mg/kg body weight/day) for 6 days. Vorinostat treatment significantly reduced the number of seizures (two-way ANOVA, $F = 27.7$, $P < 0.01$). (**C**) Acute (30 min dosing regimen) vorinostat (100 and 300 mg/kg) administration significantly reduced corneal electrode-stimulated seizures by 50 and 75%, respectively. A 2-h dosing regimen effectively reduced seizures across all concentrations used in the 6 Hz psychomotor test but not in the maximum electroshock test.

notion that combined inhibition of HDAC1 and HDAC3 might represent a set of novel anti-seizure targets.

Discussion

Here, we report a novel, metabolism-based phenotypic drug screening platform that has the potential to uncover novel molecular targets relevant for future drug design in epilepsy. We showed that both a pharmacological-induction approach and a targeted knockdown model resulted in phenotypes consistent with an 'epileptic' brain. We then characterized the metabolic profiles in these two models and demonstrated that our bioenergetics assay uncovered 18/20 current ASDs, illustrating the robustness of our approach and perhaps the translatability as well. After conducting a screen of 870 compounds, we identified vorinostat as a potent ASD and further showed that selective HDAC1 and HDAC3 inhibition might represent efficacious targets for future drug discovery. Combined, we propose that our screening approach has the potential to make significant inroads in identifying novel therapies that will be effective in epileptic patients, including the 30–40% who fail to respond to any currently available ASD.

Our novel thesis is that drugs capable of correcting derangements in metabolic output will help treat symptoms of disease. Backed by the clinical efficacy of the ketogenic diet and the growing body of evidence linking the ketogenic diet to fundamental bioenergetics processes, notably within mitochondria (Waldbaum and Patel, 2010; Milder and Patel, 2012), we reasoned that measuring mitochondrial output can serve as a proxy for overall cellular health in the background of a diseased brain. Mitochondria are the intracellular powerhouses that utilize fatty acids and glucose to create energy, and play a transformative role in cellular health. Thus, it is becoming increasingly appreciated that when mitochondria are under stress—due to ageing, lifestyle, or genetic causes—mitochondrial dysfunction can contribute to the onset of disease (Nunnari and Suomalainen, 2012). Indeed, many metabolic and nervous system disorders, as well as cancers, have now been linked to mitochondrial health. Furthermore, within

Table 1 Zinc-dependent HDACs

Compound	Class I				Class IIa				Class IIb		Class IV
	HDACI	HDAC2	HDAC3	HDAC8	HDAC4	HDAC5	HDAC7	HDAC9	HDAC6	HDAC10	HDAC11
Tacedinaline	+	–	–	–	–	–	–	–	–	–	–
MC1568	+	–	–	–	–	–	–	–	–	–	–
Pyroamide	+	–	–	–	–	–	–	–	–	–	–
Romidepsin	+	+	–	–	–	–	–	–	–	–	–
CUCD-907	+	+	–	–	–	–	–	–	–	–	–
Entinostat	+	–	+	–	–	–	–	–	–	–	–
RG2833	+	–	+	–	–	–	–	–	–	–	–
SBHA	+	–	+	–	–	–	–	–	–	–	–
RGFP 966	–	–	+	–	–	–	–	–	–	–	–
45C-202	+	+	+	–	–	–	–	–	–	–	–
BG45	+	+	+	–	–	–	–	–	–	–	–
Resminostat	+	–	+	–	–	–	–	–	+	–	–
Tasquinimod	–	–	–	–	+	–	–	–	–	–	–
LMK-235	–	–	–	–	+	+	–	–	–	–	–
Rocilinostat	–	–	–	–	–	–	–	–	+	–	–
BRD 73994	–	–	–	+	–	–	–	–	+	–	–
Droxinostat	–	–	+	+	–	–	–	–	+	–	–
Mocetinostat	+	+	+	–	–	–	–	–	–	–	+
PCI-34051	+	–	–	+	–	–	–	–	+	+	–
PCI-24781	+	+	+	+	–	–	–	–	+	+	–
VPA	+	+	+	+	+	+	+	+	–	–	–
Pracinostat	+	+	+	+	+	+	+	+	–	+	+
Trichostatin A	+	+	+	–	+	+	+	+	+	+	+
CUDC-101	+	+	+	+	+	+	+	+	+	+	+
Quisinostat	+	+	+	+	+	+	+	+	+	+	+
Belinostat	+	+	+	+	+	+	+	+	+	+	+
Vorinostat	+	+	+	+	+	+	+	+	+	+	+

HDAC inhibitors and their specific targets used for the systematic bioenergetics screen in *kcna1*-MO are presented.

neurons, mitochondria are necessary to supply large amounts of ATP and also the intermediates that are the backbone of GABA and glutamate synthesis (Sibson *et al.*, 1998; Waagepetersen *et al.*, 2001), supporting the idea that dysregulated oxidative metabolism can disrupt normal neuronal and synaptic function. Given that a complex interplay of transcription factors, hormones, co-factors, nuclear receptors, and kinases modulate mitochondrial function, broadly assaying for improvement of metabolic output in a diseased state has the potential to unbiasedly reveal disease-specific targets and/or pathways that have hitherto been under-recognized, especially in the epilepsy field. Combined, our novel approach was modelled from the current literature suggesting that mechanisms of the ketogenic diet converge to restore imbalances in energy metabolism (reviewed in Gano *et al.*, 2014) and designed to uncover overlooked molecular targets that can work upstream to stabilize mitochondrial function.

HDAC inhibitors and the treatment of epilepsy

Along these lines, our phenotypic screening platform further demonstrates that HDAC inhibition is likely an efficacious therapeutic paradigm for epilepsy. HDACs control various cellular functions by altering the dynamics of chromatin structure, which thereby affects gene transcription and can contribute to the pathogenesis of various diseases (Johnstone, 2002). The potential for HDAC inhibitors for the treatment of epilepsy was first proposed with the discovery of valproate's HDAC activity. Valproic acid is a broad ASD that is a first-line treatment for epilepsy and was originally believed to block voltage-dependent sodium channels and increase brain levels of γ-aminobutyric acid (GABA). More recently, however, valproic acid has been shown to also inhibit HDACs and it is through this action that valproic acid is thought to offer its neuroprotective effects (Gottlicher *et al.*, 2001). Vorinostat is a broad HDAC inhibitor approved by the US Food and Drug Administration for the treatment of cutaneous manifestations of cutaneous T cell lymphoma. It inhibits HDAC activity by binding in the active site of the enzyme and causes accumulation of acetylated histones, which decreases cell proliferation and inhibits tumour growth in various animal models (Richon, 2010). Interestingly, it also showed neuroprotection in epileptic animals after treatment with diazepam + vorinostat, effectively using vorinostat as a control for valproic acid HDAC activity in their experiment

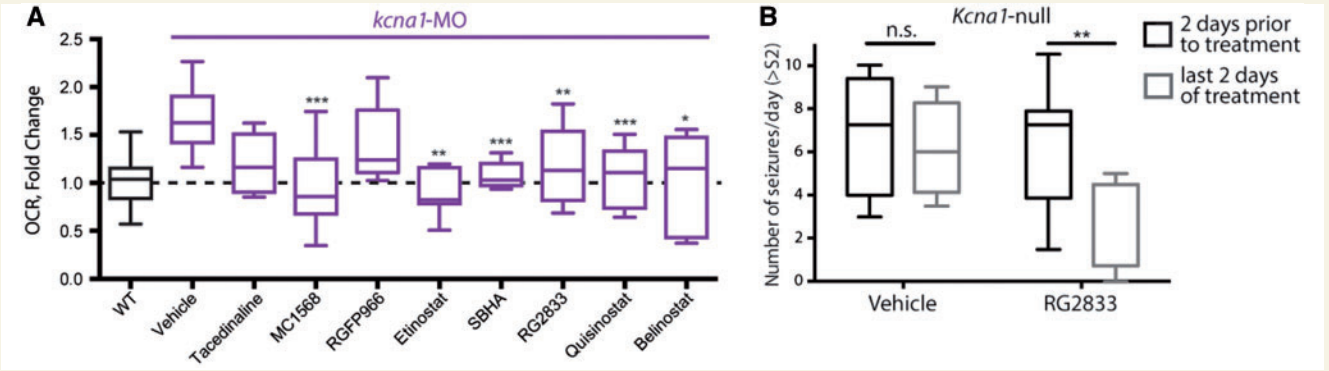

Figure 7 Inhibition of HDAC1 and HDAC3 blocks basal respiration in zebrafish. (**A**) MC1568, a HDAC1 inhibitor, reduced basal respiration in *kcna1*-MO to wild-type levels, whereas RGFP966, a selective HDAC3 inhibitor did not. Furthermore, entinostat, SBHA, and RG2833 are HDAC1 and HDAC3 inhibitors that reduced elevated basal respiration in *kcna1*-MO to wild-type levels, along with the pan-HDAC inhibitors quisinostat and belinostat. (**B**) RG2833 (100 mg/kg body weight/day) decreases the number of seizures/day following 6 days of treatment in *Kcna1*-null mice. Data in **B** and **C** are shown as mean ± SEM; $*P < 0.05$, $**P < 0.001$, $***P < 0.0001$ (unpaired *t*-test); $n = 6–7$ fish per group and $n = 4–8$ animals per group. See also Table 1.

(Rossetti *et al.*, 2012). Vorinostat inhibits both class I, IIa, IIb, IV enzymes, but not class III (Marks *et al.*, 2001; Marks and Dokmanovic, 2005). In contrast, valproic acid only inhibits class I and class IIa, perhaps suggesting that vorinostat might be even more poorly tolerated than valproic acid as a therapy. Indeed, despite considerable effort to develop HDAC inhibitors as anticancer agents, including over 490 clinical trials and three eventually approved (Li and Xu, 2014), considerable side-effects of toxicity, fatigue, nausea, vomiting, and neutropaenia have limited their utility in the clinic (Tan *et al.*, 2010). Thus, we proceeded to test selective HDAC inhibitors in an attempt to restrict the toxicity profile of this target as a potential therapy, and demonstrate that HDAC1 and HDAC3 inhibition alone can decrease the daily number of seizures in a genetic model of epilepsy. Currently, a phase I clinical trial for a HDAC1/HDAC3 selective dual inhibitor is ongoing for Friedreich's ataxia, demonstrating the potential therapeutic utility of this target in neurological disorders (Jacoby *et al.*, 2014).

Furthermore, in alignment with the rationale that the ketosis resulting from the ketogenic diet is somehow driving the improvements in overall neuronal health, recently the ketone body D-β-hydroxybutyrate was shown to be an endogenous and potent inhibitor of class I HDACs, including HDAC1 and HDAC3, which offered protection against oxidative stress in mice (Shimazu *et al.*, 2013). This is consistent with the improvement in neurological functions observed in zebrafish embryos that harbour defects in pyruvate dehydrogenase complex that were treated with ketone bodies (Taylor *et al.*, 2004). Derangements in metabolism have been demonstrated in rodent (Rowley and Patel, 2013; Kim *et al.*, 2015) and zebrafish (Kumar *et al.*, 2016) models of epilepsy, and treatment with high fatty acid diets (that generate ketone bodies) or ketone bodies themselves have been known to improve seizure control in humans (Neal *et al.*, 2008; Freeman and Kossoff, 2010) and animal models (reviewed in Masino and Rho, 2012; Kim *et al.*, 2015). Combined, these data underscore the utility of assaying for improvements in bioenergetics in epilepsy. In doing so, here we also demonstrate that our phenotypic assay has uncovered differences in efficacy between measuring metabolic output and behavioural locomotor assays in zebrafish epilepsy models.

Repurposing drugs to increase translation to the clinic

Drugs are the mainstay of epilepsy therapy, and there is an unmet medical need to identify therapeutic agents that can help the 30–40% of patients who fail to respond to any drug. We propose that to begin to make progress on finding drugs for this refractory population, we need (i) better genetic models for the discovery and validation of drugs; and (ii) new molecular targets against which novel libraries can be designed. Our lab's strategy is to harness the power of zebrafish genetics to create better vertebrate models of epilepsy and then strategically screen repurposed libraries with the intent of reverse-identifying novel molecular targets, and other preclinical compounds in the pipeline. Here, we chose to use two libraries of approved drugs, with the ultimate goal of speeding up the translation from discovery to the clinic. This approach has been widely used, primarily by academics (Oprea *et al.*, 2011), and has the distinct advantages of often enabling a phase IIa or phase IIb clinical trial, bypassing years of preclinical and phase I safety profiling. In addition, using clinically tested compounds in drug screening allows researchers to capitalize on previous investments. Of course, the restricted commercial application of discovered compounds is a limitation, but with refined *in silico* programs now available, this concern may be circumvented with the design of similar but novel compounds.

For us, the use of a repurposed library had the distinct advantage of enabling us to reverse-identify unexpected

molecular targets, against which further drug design can be leveraged. Because our readout assays are non-biased and not tied to a particular protein, and we assay for drugs that modulate mitochondrial function either directly or indirectly, we are poised to uncover new targets. Subsequently, by purchasing other commercially available inhibitors, we can easily validate these targets for future target-directed drug design. For example, from our current screen, we discovered six lead compounds (vorinostat being one), for which four compounds activated novel pathways. Thus, we propose that our screening platform not only uncovers drugs that can be exploited for future drug design, but also unexpected pathways against which targeted drug discovery could be used.

For a screening assay such as the one reported herein that begins with zebrafish models, the demonstration of translation back to mammals, especially humans, is required. To begin to translate our findings to mammals, we relied on epileptic *Kcna1*-null mice (Smart *et al.*, 1998; Rho *et al.*, 1999; Fenoglio-Simeone *et al.*, 2009) and the fact that mutations in the human homologue gene, *KCNA1*, cause spontaneous seizures in humans (Zuberi *et al.*, 1999). Using this approach, we have shown that vorinostat can reduce the number of daily seizures by 60% in *Kcna1*-null mice. In addition, we have collaborated with the NIH-sponsored ETSP to assay our top six leads across their 19 models of epilepsy. In contrast to our genetic knockout mice that exhibit spontaneous seizures, ETSP relies on acute electrical or pharmacological induction of seizures. Interestingly, vorinostat showed efficacy in both genetic and induction models, suggesting a robust clinical use for this drug that should be further tested in humans. It is worth noting that vorinostat displayed a different time course of action in the zebrafish morphants than in the mouse genetic models. Specifically, days of injection were required in the *Kcna1*-null mouse model, consistent with a potential epigenetic mechanism, whereas the effect was almost immediate in the zebrafish assays. One potential explanation for this difference is that brain concentrations of vorinostat might be higher in the zebrafish given the route of administration through the gills and skin that could bypass gut metabolism and even the blood–brain barrier, and potentially lead to non-specific effects in the brain. Alternatively, vorinostat's effects on bioenergetics (as measured in the zebrafish) and spontaneous seizures (as measured in the mouse) could be acting through different mechanisms, and thus displaying different time courses of action. Although additional experiments are needed to determine between these two scenarios (not mutually exclusive), it is important to note that a different drug (not a HDAC inhibitor but a well-characterized ASD) in our screen displayed the opposite effect, whereas it took over 8 h to show efficacy in our zebrafish models but acted almost immediately in a mouse assay (data not shown), thereby suggesting that the time course of action might not always align between the two species for reasons not well understood.

Functional readout assays for screening epileptic zebrafish larvae

To date, locomotion tracking in zebrafish has been an established readout of 'seizure behaviour', with clonus-like convulsive episodes followed by rapid hyperactive movement and then a brief pause reminiscent of post-ictal freezing (Baraban *et al.*, 2005). Thus, a decrease in locomotion in epileptic zebrafish is thought to signal an improvement in repeated episodes of convulsive-type (Stage 3 in rodents) activity. In fact, this behavioural assay is used by many labs worldwide to discover new ASDs (Berghmans *et al.*, 2007; Baxendale *et al.*, 2012; Dinday and Baraban, 2015), resulting in the first 'aquarium-to-clinic' trial (Griffin *et al.*, 2017). In contrast, here we present an assay that measures mitochondrial respiration as a readout of neuronal hyperexcitability. Therefore, a decrease in basal respiration in our epileptic zebrafish larvae to baseline levels observed in wild-type animals is an indication that mitochondrial function has stabilized. Both of these approaches have valid scientific reasoning behind them; although what is interesting is that we found no predictive correlation between these two. For example, in our epileptic zebrafish larvae, drugs that decreased locomotion did not necessarily decrease basal respiration and vice versa. This inconsistency between these two assays is perhaps surprising given that epileptic zebrafish larvae have been shown to have alterations in bioenergetics (Kumar *et al.*, 2016), and suggests that mechanisms underlying behavioural locomotion in epileptic zebrafish larvae do not involve mitochondrial changes. Further studies are required to determine if the pathophysiology underlying increased locomotion in epileptic zebrafish models correlates with 'seizures' *per se*, or instead a generalizable hyperexcitable phenotype.

The impact of genetics on drug discovery in 'epileptic' zebrafish

Epilepsy is a heterogenous disease, with both genetic and environmental factors contributing to its aetiology. Indeed, various sequencing projects in typical and refractory epilepsy are starting to shed insight into the complex genetics underlying this disorder. At the same time, the development of gene editing tools (e.g. CRISPR technology) make it now possible to create a seemingly limitless number of mouse and zebrafish genetic models to both better understand the underlying aetiology of epilepsy and also to use in drug screening. Although the advancements from these models will be significant, it does raise the question as to whether drug screening in individual genetic models will yield drugs that are efficacious in only that genetic background, or will be more widely useful. Here, we demonstrate striking differences between PTZ-induction and *kcna1*-MO, although our comparison between *kcna1*-MO and other genetic models created in the lab shows similarity across genetic lines and dissimilarity between induction and knockout

models (unpublished results). Although future work is needed, it is tempting to speculate that an underlying genetic aetiology of epilepsy will affect the cellular milieu differently than modulating hyperexcitability at the synapse (e.g. via treatment with PTZ or electric current), and perhaps makes an argument for using genetic lines in drug screening. Our platform allows us to test this notion directly by comparing efficacy of different drugs across multiple models, genetic and induction. By keeping the readout assays the same and simply changing the zebrafish epilepsy model, we can ask whether drugs behave similarly across different genetic backgrounds, and also obtain evidence as to whether a drug might be equally efficacious across a broad population or specific to a particular genetic cause. And finally, our screening platform allows us to make genetic models of rare epilepsies, for which no therapeutic options exist. This approach can be of benefit especially to paediatric epilepsy populations, which usually suffer the most severe monogenic epilepsies.

A limitation of our study is the use of MOs as our zebrafish knockdown model, instead of CRISPR-associated systems (CRISPR/cas9)-generated mutants. MOs are injected at the one-cell stage and bind tightly to the target sequence to block translation of protein, and are thereby considered a knockdown (versus knockout) approach. With the advent of CRISPRs, the popularity of MOs has decreased; however, laboratories worldwide are starting to report a lack of phenotype in many CRISPR/cas9-generated mutants, especially when compared with earlier studies conducted with MOs (Schulte-Merker and Stainier, 2014; Kok *et al.*, 2015). This lack of phenotype is proposed to be due to compensation by other genes as the embryo seeks to maintain homeostasis (Schulte-Merker and Stainier, 2014). Thus, although we have since gone on to create CRISPR zebrafish mutants for all future drug discovery (Meza Santoscoy *et al.*, in preparation), our strategy herein was to develop this proof-of-principle platform using MOs that we have demonstrated to have robust and reproducible spontaneous seizure phenotype in larval zebrafish. All future drug screening take place using our newly characterized CRISPR/cas9 'epileptic' zebrafish lines.

Conclusion

In conclusion, we describe a novel drug screening platform that relies on bioenergetics to identify new molecular targets for the treatment of epilepsy. We found that vorinostat can decrease seizures in both genetic and induction models of epilepsy, and propose combined HDAC1 and HDAC3 inhibition as a novel anti-seizure paradigm. Further, we suggest that our unbiased screening platform can be utilized across a variety of CNS disorders for which alterations in mitochondrial function have been implicated, by simply creating disease-relevant and gene-specific zebrafish mutants and using a similar workflow.

Acknowledgements

We would like to thank Dr Aru Narendran for kindly sharing his 142 compound chemical library and Dr Timothy Simeone (Creighton University) for providing *Kcna1*$^{+/-}$ breeders. We also acknowledge the Epilepsy Therapy Screening Program for their assistance in screening our compounds, especially Dr Steve White (University of Washington, Seattle). We also thank Elizabeth Hughes for assistance with mouse husbandry and genotyping and Younghee Ahn for training and support on the Seahorse Bioanalyzer. Finally, we thank Alicia Vandenbrink and Rose Tobias for administrative support.

Funding

This work was funded by Brain Canada Platform Support Grant to D.M.K. and J.M.R. and the Alberta Children's Hospital Foundation and the Alberta Children's Hospital Research Institute for seed funding, as well as Barrow Neurological Foundation to D.Y.K.

Conflicts of interest

The authors declare no competing interests. An International Patent (Application PCT/IB2015/000644) has been filed by K.I., J.M.R., and D.M.K. that includes some of the data herein. For a portion of the project duration, J.M.R. served as a paid consultant to Accera Pharmaceuticals, Eisai Canada, UCB Canada, and Xenon Pharmaceuticals; none of the results contained herein reflect a conflict with these organizations.

Supplementary material

Supplementary material is available at *Brain* online.

References

Abdelwahab MG, Fenton KE, Preul MC, Rho JM, Lynch A, Stafford P, et al. The ketogenic diet is an effective adjuvant to radiation therapy for the treatment of malignant glioma. PLoS One 2012; 7: e36197.

Acharya MM, Hattiangady B, Shetty AK. Progress in neuroprotective strategies for preventing epilepsy. Prog Neurobiol 2008; 84: 363–404.

Afrikanova T, Serruys AS, Buenafe OE, Clinckers R, Smolders I, de Witte PA, et al. Validation of the zebrafish pentylenetetrazol seizure model: locomotor versus electrographic responses to antiepileptic drugs. PLoS One 2013; 8: e54166.

Baraban SC, Dinday MT, Castro PA, Chege S, Guyenet S, Taylor MR. A large-scale mutagenesis screen to identify seizure-resistant zebrafish. Epilepsia 2007; 48: 1151–7.

Baraban SC, Dinday MT, Hortopan GA. Drug screening in Scn1a zebrafish mutant identifies clemizole as a potential Dravet syndrome treatment. Nat Commun 2013; 4: 2410.

Baraban SC, Taylor MR, Castro PA, Baier H. Pentylenetetrazole induced changes in zebrafish behavior, neural activity and c-fos expression. Neuroscience 2005; 131: 759–68.
Barton ME, Klein BD, Wolf HH, White HS. Pharmacological characterization of the 6 Hz psychomotor seizure model of partial epilepsy. Epilepsy Res 2001; 47: 217–27.
Barton ME, Peters SC, Shannon HE. Comparison of the effect of glutamate receptor modulators in the 6 Hz and maximal electroshock seizure models. Epilepsy Res 2003; 56: 17–26.
Baxendale S, Holdsworth CJ, Meza Santoscoy PL, Harrison MR, Fox J, Parkin CA, et al. Identification of compounds with anti-convulsant properties in a zebrafish model of epileptic seizures. Dis Model Mech 2012; 5: 773–84.
Berg AT, Testa FM, Levy SR, Shinnar S. The epidemiology of epilepsy. Past, present, and future. Neurol Clin 1996; 14: 383–98.
Berghmans S, Hunt J, Roach A, Goldsmith P. Zebrafish offer the potential for a primary screen to identify a wide variety of potential anticonvulsants. Epilepsy Res 2007; 75: 18–28.
Bouilleret V, Ridoux V, Depaulis A, Marescaux C, Nehlig A, Le Gal La Salle G. Recurrent seizures and hippocampal sclerosis following intrahippocampal kainate injection in adult mice: electroencephalography, histopathology and synaptic reorganization similar to mesial temporal lobe epilepsy. Neuroscience 1999; 89: 717–29.
Bromley RL, Leeman BA, Baker GA, Meador KJ. Cognitive and neurodevelopmental effects of antiepileptic drugs. Epilepsy Behav 2011; 22: 9–16.
Davis LM, Pauly JR, Readnower RD, Rho JM, Sullivan PG. Fasting is neuroprotective following traumatic brain injury. J Neurosci Res 2008; 86: 1812–22.
Dinday MT, Baraban SC. Large-scale phenotype–based antiepileptic drug screening in a zebrafish model of dravet syndrome(1,2,3). eNeuro 2015; 2.
Evangeliou A, Vlachonikolis I, Mihailidou H, Spilioti M, Skarpalezou A, Makaronas N, et al. Application of a ketogenic diet in children with autistic behavior: pilot study. J Child Neurol 2003; 18: 113–18.
Fenoglio-Simeone KA, Wilke JC, Milligan HL, Allen CN, Rho JM, Maganti RK. Ketogenic diet treatment abolishes seizure periodicity and improves diurnal rhythmicity in epileptic Kcna1-null mice. Epilepsia 2009; 50: 2027–34.
Freeman JM, Kossoff EH. Ketosis and the ketogenic diet, 2010: advances in treating epilepsy and other disorders. Adv Pediatr 2010; 57: 315–29.
Frye RE, Sreenivasula S, Adams JB. Traditional and non-traditional treatments for autism spectrum disorder with seizures: an on-line survey. BMC Pediatr 2011; 11: 37.
Gano LB, Patel M, Rho JM. Ketogenic diets, mitochondria, and neurological diseases. J Lipid Res 2014; 55: 2211–28.
Gasior M, Rogawski MA, Hartman AL. Neuroprotective and disease-modifying effects of the ketogenic diet. Behav Pharmacol 2006; 17: 431–9.
Gibert Y, McGee SL, Ward AC. Metabolic profile analysis of zebrafish embryos. J Vis Exp 2013: e4300.
Gottlicher M, Minucci S, Zhu P, Kramer OH, Schimpf A, Giavara S, et al. Valproic acid defines a novel class of HDAC inhibitors inducing differentiation of transformed cells. EMBO J 2001; 20: 6969–78.
Greco T, Glenn TC, Hovda DA, Prins ML. Ketogenic diet decreases oxidative stress and improves mitochondrial respiratory complex activity. J Cereb Blood Flow Metab 2016; 36: 1603–13.
Griffin A, Hamling KR, Knupp K, Hong S, Lee LP, Baraban SC. Clemizole and modulators of serotonin signalling suppress seizures in Dravet syndrome. Brain 2017; 40: 669–83.
Grone BP, Marchese M, Hamling KR, Kumar MG, Krasniak CS, Sicca F, et al. Epilepsy, behavioral abnormalities, and physiological comorbidities in syntaxin-binding protein 1 (STXBP1) mutant zebrafish. PLoS One 2016; 11: e0151148.
Henderson ST, Vogel JL, Barr LJ, Garvin F, Jones JJ, Costantini LC. Study of the ketogenic agent AC-1202 in mild to moderate Alzheimer's disease: a randomized, double-blind, placebo-controlled, multicenter trial. Nutr Metab 2009; 6: 31.
Herbert MR, Buckley JA. Autism and dietary therapy: case report and review of the literature. J Child Neurol 2013; 28: 975–82.
Howe K, Clark MD, Torroja CF, Torrance J, Berthelot C, Muffato M, et al. The zebrafish reference genome sequence and its relationship to the human genome. Nature 2013; 496: 498–503.
Jacoby D, Rusche J, Iudicello M, De Mercanti S, Clerico M, Gibbin M, et al. Epigenetic therapy for Friedreich's ataxia: a phase I clinical trial (PL1.003). Neurology 2014; 82 (10 Supplement).
Johnstone RW. Histone-deacetylase inhibitors: novel drugs for the treatment of cancer. Nat Rev Drug Discov 2002; 1: 287–99.
Kang HC, Lee YM, Kim HD, Lee JS, Slama A. Safe and effective use of the ketogenic diet in children with epilepsy and mitochondrial respiratory chain complex defects. Epilepsia 2007; 48: 82–8.
Kanner AM. Do psychiatric comorbidities have a negative impact on the course and treatment of seizure disorders? Curr Opin Neurol 2013a; 26: 208–13.
Kanner AM. The treatment of depressive disorders in epilepsy: what all neurologists should know. Epilepsia 2013b; 54 (Suppl 1): 3–12.
Kettleborough RN, Busch-Nentwich EM, Harvey SA, Dooley CM, de Bruijn E, van Eeden F, et al. A systematic genome-wide analysis of zebrafish protein-coding gene function. Nature 2013; 496: 494–7.
Kim do Y, Hao J, Liu R, Turner G, Shi FD, Rho JM. Inflammation-mediated memory dysfunction and effects of a ketogenic diet in a murine model of multiple sclerosis. PLoS One 2012; 7: e35476.
Kim DY, Simeone KA, Simeone TA, Pandya JD, Wilke JC, Ahn Y, et al. Ketone bodies mediate antiseizure effects through mitochondrial permeability transition. Ann Neurol 2015; 78: 77–87.
Kok FO, Shin M, Ni CW, Gupta A, Grosse AS, van Impel A, et al. Reverse genetic screening reveals poor correlation between morpholino-induced and mutant phenotypes in zebrafish. Dev Cell 2015; 32: 97–108.
Kossoff EH, Rho JM. Ketogenic diets: evidence for short- and long-term efficacy. Neurotherapeutics 2009; 6: 406–14.
Kossoff EH, Zupec-Kania BA, Amark PE, Ballaban-Gil KR, Christina Bergqvist AG, Blackford R, et al. Optimal clinical management of children receiving the ketogenic diet: recommendations of the International Ketogenic Diet Study Group. Epilepsia 2009; 50: 304–17.
Kumar MG, Rowley S, Fulton R, Dinday MT, Baraban SC, Patel M. Altered glycolysis and mitochondrial respiration in a zebrafish model of Dravet syndrome. eNeuro 2016; 3.
Kwan P, Brodie MJ. Early identification of refractory epilepsy. N Engl J Med 2000; 342: 314–9.
Li X, Xu W. HDAC1/3 dual selective inhibitors—new therapeutic agents for the potential treatment of cancer. Drug Discov Ther 2014; 8: 225–8.
Linehan C, Tellez-Zenteno JF, Burneo JG, Berg AT. Future directions for epidemiology in epilepsy. Epilepsy Behav 2011; 22: 112–7.
Loscher W, Schmidt D. Modern antiepileptic drug development has failed to deliver: ways out of the current dilemma. Epilepsia 2011; 52: 657–78.
Maalouf M, Rho JM, Mattson MP. The neuroprotective properties of calorie restriction, the ketogenic diet, and ketone bodies. Brain Res Rev 2009; 59: 293–315.
Maggioni F, Margoni M, Zanchin G. Ketogenic diet in migraine treatment: a brief but ancient history. Cephalalgia 2011; 31: 1150–1.
Marks PA, Dokmanovic M. Histone deacetylase inhibitors: discovery and development as anticancer agents. Expert Opin Investig Drugs 2005; 14: 1497–511.
Marks PA, Richon VM, Breslow R, Rifkind RA. Histone deacetylase inhibitors as new cancer drugs. Curr Opin Oncol 2001; 13: 477–83.
Maroon J, Bost J, Amos A, Zuccoli G. Restricted calorie ketogenic diet for the treatment of glioblastoma multiforme. J Child Neurol 2013; 28: 1002–8.
Masino SA, Kawamura M, Wasser CD, Pomeroy LT, Ruskin DN. Adenosine, ketogenic diet and epilepsy: the emerging therapeutic

relationship between metabolism and brain activity. Curr Neuropharmacol 2009; 7: 257–68.
Masino SA, Rho JM. Mechanisms of ketogenic diet action. In: Noebels JL, Avoli M, Rogawski MA, Olsen RW, Delgado-Escueta AV, editors. Jasper's basic mechanisms of the epilepsies. 4th edn. Bethesda, MD: Oxford University Press; 2012.
Meyer M, Dhamne SC, LaCoursiere CM, Tambunan D, Poduri A, Rotenberg A. Correction: microarray noninvasive neuronal seizure recordings from intact larval zebrafish. PLoS One 2016; 11: e0159472.
Milder J, Patel M. Modulation of oxidative stress and mitochondrial function by the ketogenic diet. Epilepsy Res 2012; 100: 295–303.
Mula M. Treatment of anxiety disorders in epilepsy: an evidence-based approach. Epilepsia 2013; 54 (Suppl 1): 13–8.
Neal EG, Chaffe H, Schwartz RH, Lawson MS, Edwards N, Fitzsimmons G, et al. The ketogenic diet for the treatment of childhood epilepsy: a randomised controlled trial. Lancet Neurol 2008; 7: 500–6.
Neal EG, Chaffe H, Schwartz RH, Lawson MS, Edwards N, Fitzsimmons G, et al. A randomized trial of classical and medium-chain triglyceride ketogenic diets in the treatment of childhood epilepsy. Epilepsia 2009; 50: 1109–17.
Neligan A, Hauser W, Sander JW. The epidemiology of the epilepsies. Handb Clin Neurol 2012; 107: 113–33.
Nunnari J, Suomalainen A. Mitochondria: in sickness and in health. Cell 2012; 148: 1145–59.
Oprea TI, Bauman JE, Bologa CG, Buranda T, Chigaev A, Edwards BS, et al. Drug repurposing from an academic perspective. Drug Discov Today Ther Strateg 2011; 8: 61–9.
Pathak D, Berthet A, Nakamura K. Energy failure: does it contribute to neurodegeneration? Ann Neurol 2013; 74: 506–16.
Phelps JR, Siemers SV, El-Mallakh RS. The ketogenic diet for type II bipolar disorder. Neurocase 2012.
Rho JM, Szot P, Tempel BL, Schwartzkroin PA. Developmental seizure susceptibility of kv1.1 potassium channel knockout mice. Dev Neurosci 1999; 21: 320–7.
Riban V, Bouilleret V, Pham-Le BT, Fritschy JM, Marescaux C, Depaulis A. Evolution of hippocampal epileptic activity during the development of hippocampal sclerosis in a mouse model of temporal lobe epilepsy. Neuroscience 2002; 112: 101–11.
Richon VM. Targeting histone deacetylases: development of vorinostat for the treatment of cancer. Epigenomics 2010; 2: 457–65.
Rogawski MA, Loscher W, Rho JM. Mechanisms of action of antiseizure drugs and the ketogenic diet. Cold Spring Harb Perspect Med 2016; 6.
Rossetti F, de Araujo Furtado M, Pak T, Bailey K, Shields M, Chanda S, et al. Combined diazepam and HDAC inhibitor treatment protects against seizures and neuronal damage caused by soman exposure. Neurotoxicology 2012; 33: 500–11.
Rowley S, Patel M. Mitochondrial involvement and oxidative stress in temporal lobe epilepsy. Free Radic Biol Med 2013; 62: 121–31.
Rudzinshi L, Meador K. Epilepsy and neuropsychological comorbidities. Continuum 2013; 19 (3 (Epilepsy): 682–96.
Ruskin DN, Svedova J, Cote JL, Sandau U, Rho JM, Kawamura M Jr, et al. Ketogenic diet improves core symptoms of Autism in BTBR mice. PLoS One 2013; 8: e65021.
Schier AF. Genomics: zebrafish earns its stripes. Nature 2013; 496: 443–4.
Schmidt M, Pfetzer N, Schwab M, Strauss I, Kammerer U. Effects of a ketogenic diet on the quality of life in 16 patients with advanced cancer: a pilot trial. Nutr Metab 2011; 8: 54.
Schulte-Merker S, Stainier DY. Out with the old, in with the new: reassessing morpholino knockdowns in light of genome editing technology. Development 2014; 141: 3103–4.
Shimazu T, Hirschey MD, Newman J, He W, Shirakawa K, Le Moan N, et al. Suppression of oxidative stress by beta-hydroxybutyrate, an endogenous histone deacetylase inhibitor. Science 2013; 339: 211–4.
Sibson NR, Dhankhar A, Mason GF, Rothman DL, Behar KL, Shulman RG. Stoichiometric coupling of brain glucose metabolism and glutamatergic neuronal activity. Proc Natl Acad Sci USA 1998; 95: 316–21.
Smart SL, Lopantsev V, Zhang CL, Robbins CA, Wang H, Chiu SY, et al. Deletion of the K(V)1.1 potassium channel causes epilepsy in mice. Neuron 1998; 20: 809–19.
Stackley KD, Beeson CC, Rahn JJ, Chan SS. Bioenergetic profiling of zebrafish embryonic development. PLoS One 2011; 6: e25652.
Stafford P, Abdelwahab MG, Kim do Y, Preul MC, Rho JM, Scheck AC. The ketogenic diet reverses gene expression patterns and reduces reactive oxygen species levels when used as an adjuvant therapy for glioma. Nutr Metab 2010; 7: 74.
Stafstrom CE, Rho JM. The ketogenic diet as a treatment paradigm for diverse neurological disorders. Front Pharmacol 2012; 3: 59.
Suzuki F, Junier MP, Guilhem D, Sorensen JC, Onteniente B. Morphogenetic effect of kainate on adult hippocampal neurons associated with a prolonged expression of brain-derived neurotrophic factor. Neuroscience 1995; 64: 665–74.
Suzuki S, Kawakami K, Nishimura S, Watanabe Y, Yagi K, Seino M, et al. Zonisamide blocks T-type calcium channel in cultured neurons of rat cerebral cortex. Epilepsy Res 1992; 12: 21–7.
Tan J, Cang S, Ma Y, Petrillo RL, Liu D. Novel histone deacetylase inhibitors in clinical trials as anti-cancer agents. J Hematol Oncol 2010; 3: 5.
Taylor MR, Hurley JB, Van Epps HA, Brockerhoff SE. A zebrafish model for pyruvate dehydrogenase deficiency: rescue of neurological dysfunction and embryonic lethality using a ketogenic diet. Proc Natl Acad Sci USA 2004; 101: 4584–9.
Waagepetersen HS, Sonnewald U, Gegelashvili G, Larsson OM, Schousboe A. Metabolic distinction between vesicular and cytosolic GABA in cultured GABAergic neurons using 13C magnetic resonance spectroscopy. J Neurosci Res 2001; 63: 347–55.
Waldbaum S, Patel M. Mitochondrial dysfunction and oxidative stress: a contributing link to acquired epilepsy? J Bioenerg Biomembr 2010; 42: 449–55.
Westerfield M. The zebrafish book. A guide for the laboratory use of zebrafish (Danio Rerio). 4th edn. Eugene: University of Oregon Press; 2000.
White HS, Johnson M, Wolf HH, Kupferberg HJ. The early identification of anticonvulsant activity: role of the maximal electroshock and subcutaneous pentylenetetrazol seizure models. Ital J Neurol Sci 1995; 16: 73–7.
Winter MJ, Redfern WS, Hayfield AJ, Owen SF, Valentin JP, Hutchinson TH. Validation of a larval zebrafish locomotor assay for assessing the seizure liability of early-stage development drugs. J Pharmacol Toxicol Methods 2008; 57: 176–87.
Yaroslavsky Y, Stahl Z, Belmaker RH. Ketogenic diet in bipolar illness. Bipolar Disord 2002; 4: 75.
Zdebik AA, Mahmood F, Stanescu HC, Kleta R, Bockenhauer D, Russell C. Epilepsy in kcnj10 morphant zebrafish assessed with a novel method for long-term EEG recordings. PLoS One 2013; 8: e79765.
Zuberi SM, Eunson LH, Spauschus A, De Silva R, Tolmie J, Wood NW, et al. A novel mutation in the human voltage-gated potassium channel gene (Kv1.1) associates with episodic ataxia type 1 and sometimes with partial epilepsy. Brain 1999; 122 (Pt 5): 817–25.